

Quantum Walks with Bipartite Entangled Coins



Saba Arshad
Regn.#365384

A thesis submitted in partial fulfillment of the requirements
for the degree of **Master of Science**
in
Physics

Supervised by: Prof. Dr. Shahid Iqbal

Department of Physics
School of Natural Sciences
National University of Sciences and Technology
H-12, Islamabad, Pakistan

2023

THESIS ACCEPTANCE CERTIFICATE

Certified that final copy of MS thesis written by Saba Arshad (Registration No. 00000365384), of School of Natural Sciences has been vetted by undersigned, found complete in all respects as per NUST statutes/regulations, is free of plagiarism, errors, and mistakes and is accepted as partial fulfillment for award of MS/M.Phil degree. It is further certified that necessary amendments as pointed out by GEC members and external examiner of the scholar have also been incorporated in the said thesis.


Signature: 

Name of Supervisor: Prof. Shahid Iqbal

Date: 06/07/2023

Signature (HoD): 


Date: 06-07-2023

Signature (Dean/Principal): 

Date: 6/7/23

National University of Sciences & Technology**MS THESIS WORK**

We hereby recommend that the dissertation prepared under our supervision by: Saba Arshad, Regn No. 00000365384 Titled: Quantum Walks with Bipartite Entangled Coins be Accepted in partial fulfillment of the requirements for the award of **MS** degree.

Examination Committee Members1. Name: Dr. NAILA AMIRSignature:  _____2. Name: DR. MUHAMMAD ALI PARACHASignature:  _____Supervisor's Name PROF. SHAHID IQBALSignature:  _____



 Head of Department

06-07-2023

 Date

COUNTERSIGNEDDate: 6/7/23



 Dean/Principal

Dedication

This thesis is dedicated *to my beloved parents.*

Acknowledgements

In the beginning, I would like to pay thanks to Allah, the All-Powerful and the Most Merciful, for the blessing that He has bestowed upon me throughout my studies and in the process of finishing my thesis. I would like to pay regards to my esteemed supervisor Prof. Dr. Shahid Iqbal for his impeccable supervision, tutelage and support during the term of my research. I am thankful to him for his insightful feedback, expertise and methodology that helped sharpen my thinking. I am forever grateful to my parents for their guidance, sympathetic ear and financial support. Lastly, this work couldn't have reached its completion without the support of my friends, who extended helpful discussions and joyous distractions to rest my mind outside of research.

Abstract

The Quantum Walk is the quantum version of classical random walk. In a conventional "Discrete-time Quantum Walk (DTQW)", coin and shift unitary operators guide the evolution of the walker after some steps. While the direction of motion is determined by the coin operator, the shift operator displaces the walker's position by one or more unit steps to the right or left. In this thesis, we have highlighted the important measures to inquire the degree of entanglement in discrete and bipartite system. Entanglement of particles is a predominant aspect of quantum mechanical systems and is the most contradictory with classical intuitions. The use of entanglement as a resource is explored in the computational tool of quantum walks wherein, entanglement in the coin states enhances the probability distribution of the walker to far off positions. This is exploited to devise quantum algorithms that are much fast paced as compared to their classical counterparts. Applications include secure quantum key distribution in cryptography, super-dense coding, teleportation, etc and the most striking implementation in quantum computers which make use of entangled bits as data registers for faster processing of information.

Contents

1	Introduction	1
1.1	Preamble	1
1.2	Preliminary Introduction	2
1.3	Discipline of Study	4
2	Preliminaries	6
2.1	Quantum Bit	6
2.2	Quantum Systems	8
2.3	Density Operator	8
2.4	Categorization of States	10
2.4.1	Pure State	10
2.4.2	Mixed State	10
2.5	Entanglement	11
2.5.1	Quantification of Entanglement	11
2.6	Maximally Entangled State	15
2.6.1	Generation Of Bell States	15
3	Introduction to CRW and QW	17
3.1	Classical Random Walk(CRW)	17
3.1.1	Discrete-time Markov Chain	19
3.1.2	Continuous-time Markov Chain	21

3.1.3	Limitations of Classical Random Walk	23
3.2	Quantum Walk (QW)	23
3.2.1	Discrete Time Quantum Walk	24
3.2.2	Continuous Time Quantum Walk	24
3.3	Coined Quantum Walk on a line	25
3.3.1	Spin-up Coin State :	26
3.3.2	Spin-Down Coin State :	29
3.3.3	Superposition Coin State :	32
4	Quantum Walk with Bipartite Entangled Coins	35
4.1	Quantum Walk with Separable Coin State	35
4.2	Quantum Walk with Partially Entangled Coin	38
4.3	Quantum Walk with Maximally Entangled Coins	40
4.4	Quantum Walk with Complex Coefficients in the Coin initial state	48
5	Summary and Conclusion	50
	Bibliography	52

List of Figures

3.1	A classical Galton Board showing the multiple paths available for the particle.	18
3.2	Probability distribution of a classical random walk	20
3.3	The probabilities of the walker after 60,100,200,700 steps of the walk with a coin in the up spin state are plotted against the positions where the walker can be located. The right going amplitudes undergo constructive interference hence enhancing the probabilities towards the right side on the line.	28
3.4	The probabilities of the walker after 60,100,200,700 steps of the walk with a coin in the down spin state are plotted against the positions where the walker can be located. The left going amplitudes undergo destructive interference hence enhancing the probabilities towards the left side on the line.	30
3.5	The probabilities of the walker after 60, 100, 200 and 700 steps of the walk with a coin in the superposed spin state are plotted against the positions where the walker can be located.	33
4.1	Probabilities for locating the walker at various positions after 60, 100, 200 and 700 steps of the walk using a separable coin state.It reproduces a similar graph as that of spin-up coin state. It shows that the use of separable state with real coefficients distributes the probability to only one side of the graph.	37

4.2	Probabilities for locating the walker at various positions after 60, 100, 200 and 700 steps of the walk using a partially entangled coin state. . .	39
4.3	The probabilities of the walker after 60, 100 200, 700 steps of the walk with a maximally entangled coin state are plotted against the positions where the walker can be located.	42
4.4	The probabilities of the walker after 100, 200 and 500 steps of the walk with a First Bell state as coin state are plotted against the positions where the walker can be located. Coin operator for blue and green plots is given by eq.4.6 and dashed orange and red plots are given by 4.24 . .	44
4.5	The probabilities of the walker after 100 and 200 steps of the walk with a Third Bell state as coin state are plotted against the positions where the walker can be located. Coin operator for red and blue plots are given by eq.4.6 and dashed orange and green plots are given by 4.24.	46
4.6	The probabilities of the walker after 100 and 500 steps of the walk with a first Bell state (orange dashed line) and $\sqrt{0.85} 0\rangle - \sqrt{0.15} 1\rangle$ (blue dashed line) as coin states are plotted against the positions where the walker can be located. Coin operator for red and blue plots are given by eq. 4.6 and dashed orange and green plots are given by 4.24.	47
4.7	The probabilities of the walker after 100 steps of the walk with a complex coefficients in coin initial state are plotted against the positions where the walker can be located.	49

List of Tables

3.1	Probability distribution for a classical walk	19
4.1	The probability distribution of the walker with maximally entangled coin state after first three steps of the walk. It suggests that entanglement produces symmetry in the distribution.	42

Chapter 1

Introduction

1.1 Preamble

The journey from classical to quantum physics marked a groundbreaking shift in our understanding of the fundamental nature of reality. Classical physics, with its Newtonian mechanics and deterministic laws, provided a solid framework for describing the macroscopic world. The birth of quantum physics brought about a revolution, introducing the concept of wave-particle duality and the inherent uncertainty in the behavior of subatomic particles. Quantum mechanics has developed over time as a way to explain things that classical physics couldn't, like in 1900, Max Planck found a way to solve the black-body radiation problem [1] and Albert Einstein investigated the photoelectric effect in 1905 [2]. In the first quarter of the 20th century, several scientists, including Erwin Schrodinger, Werner Heisenberg, and others, finally succeeded in developing quantum mechanics because of these early efforts. Data processing has been revolutionized by the quantum physics in different areas of science, incorporating computer science and engineering. The most promising area in these fields is by and large the invention in hardware and software program instruments. As the requirement for the most efficient use of computational resources are increasing day by day, new technology, computational techniques better and efficient algorithms are emerged as significant factors. The possibility of quantum mechanics merging into the traditional computational paradigms generates the new ideas of quantization of existing algorithms. As a result of this quantization we get different quantum algorithms for

example, Shor's algorithm [6]. The process of quantization has emerged development of many quantum fields such as quantum statistics and some quantum algorithms that are related to each other. Much of the quantum formalism began to assimilate into information theory at laboratory level however, it took several decades to incorporate the soul of the quantum mechanics entanglement, into practical application as a potential resource. In compound quantum systems, entanglement is viewed as a holistic characteristic which correlates the subsystems non-classically. It is a candidate for many research advances such as quantum cryptography [3], [4], dense coding [5], quantum key distribution and teleportation [6]. Due to its fragility to the environment, the detection and quantification of entanglement gets complicated. To decipher its complex formation, many mathematical tools have been devised some of which cover the scope of this thesis.

1.2 Preliminary Introduction

In classical physics, classical random walks(CRW) are important to develop several algorithms in computer science and mathematics and applications in algorithms like building stochastic algorithms [8]. When classical random walk is combined with theoretical physics principles, it evolves a new framework i.e. quantum walks. The quantum mechanical equivalent of the classical random walk is quantum walk (QW). There are two types of quantum walks that got significant attention: continuous [8]–[13] and discrete [14]–[20] quantum walks. In this thesis, I will target discrete quantum walks. The quantum walks have been exhaustively studied in the context of quantum algorithms, graph theory, and quantum simulations, offering unique insights into non-classical regimes. The characteristic features of the quantum walk are governed by the principles of quantum mechanics. Instead of moving along a classical trajectory, the quantum walker explores a superposition of different positions simultaneously. This allows for the interference of probability amplitudes, leading to unique properties and potential advantages over classical random walks.

The use of quantum walks is in the development of new quantum algorithms. Childs

et al. [21] comes up with continuous-time quantum walk algorithm for graph connectivity and have exponential speed-up over other already present classical algorithms, whereas Shenvi et al. [22] creates a quantum algorithm that is quadratically faster for searching a marked vertex on a hypercube. In addition to previous discussion, Ambainis et al [23] proved that that quantum walks on a line demonstrate quadratic speed over classical random walks. Also it is proved by Kempe [24] that the time required by a quantum walk of a hypercube is polynomial in terms of the number of steps. Finally, the problem of element distinctness is solved by quantum algorithm which is based on quantum walk which is found in [25]. A fantastic overview of the fundamentals of quantum walks is given by [26], while [27] compiles algorithmic applications for quantum walks. A walker and a coin are the two physical systems that make up a discrete quantum walk; a comprehensive overview of these two systems is given in section 3. Numerous studies have been done on the characteristics of quantum walks by using several coin operators [28]–[30] and decoherent coins [31]–[33] to a single walker.

However, entanglement is less discussed in quantum walks. By using evolution operators that are non-separable on discrete quantum walks and their results of probability distribution and its effects on the standard deviation is given in [34], accompanied by [29] in which a more thorough investigation is given on non-separable operators. A continuous quantum walk on a circle was suggested by Du et al in [35], and it was mathematically explained that entanglement that is found in the states of the position changes the probability distribution of position. In the recent Study, [36] provides a description of models for a quantum walk on a line with two particles that are entangled, acting as quantum walkers. The entanglement between particle and coin on graphs is studied in [37], in addition to it the quantum walk algorithm is discussed in [22]. The authors examine the connection between the average location of the three and four qubit coins and coin entanglement in [38]. The entanglement that is produced by the shift operator among one coin and one walker quantum walk has also been quantified by Abal et al in [39]. We have two reasons for using entangled coins in quantum walks. First of all, employing entangled coins $|c\rangle \notin \mathcal{H}^n$ in quantum walks on graphs $G(V, E)$ with $\deg(v_j) = m \forall v_j \in V$ where $n > m$ expands the use of various shift operators in

quantum walks. Specifically, we use shift operators that allows the walker to remain at the same vertex, in this study maximally entangled coins are being used in order to perform quantum walks over an unending line. Secondly, it is possible to think of a coin with two entangled qubits that are each in the region of H^2 as a single coin that has been defined on H^4 and then suitably divided. In fact, the space H^4 is covered by the ortho-normal basis $|00\rangle, |01\rangle, |10\rangle, |11\rangle$. Entanglement, on the other hand, is a super-correlation between potential space-like separated quantum system components. There are two main applications of quantum walk known as cavity-QED based [40] and ion-trap based [41] which define the situation taken in this thesis. In both of these applications, coin is taken as two-level atoms but walker is a cavity mode [40] or a vibrational mode [41]. Two atomic qubits that exists in an ion trap are created in Bell states [42]. There are many proposed methods for entangling two atomic qubits in a cavity, such as [43]. The common ion-trap vibrational mode or the common cavity mode can therefore be utilized to represent these atoms as entangled coins, with the walker being restrained by both of the existing coins.

In this article, I'll talk about how a quantum walk behaves on an endless line, also known as an unlimited quantum walk, when there is just one walker and one coin made up of two maximally entangled particles. We evaluate how well such a walk performs in comparison to a traditional random walk with one walker and two maximally correlated coins. I also show how applying various shift operators on coins results in varied position probability distributions in one-dimensional graphs.

1.3 Discipline of Study

Our work is divided into five major sections:

- First section: This section provides preliminary introduction and background behind my research. It also explains literature review.
- Second section: This section discusses the preliminary tools of quantum mechanics, quantum composite systems, density operator and categorization of states

via density operator, entanglement, and a brief introduction on quantification of entanglement, and finally a brief discussion on Bell States.

- Third Section: It provides a basic overview of classical and quantum walk and explores discrete time quantum walk – coined quantum walk.
- Fourth Section: This section gives the detailed discussion on bipartite entangled coin. It also talks about the advantage of using entangled coins in the walk.
- Fifth Section: It features the summary of the previous sections and concludes the whole thesis. It gives the overall analysis of results that are obtained. It also focuses on future prospects.

Chapter 2

Preliminaries

2.1 Quantum Bit

The fundamental unit of information in quantum computing and quantum information theory is the quantum bit, considered as a qubit. Qubits have special features, derived from quantum mechanics, such as they process and store information similar to classical bits in classical computing. Qubits have the ability to exist in a superposition of many states simultaneously, in contrast to classical bits, which can only represent one of two states (0 or 1) [44]. A key property of quantum mechanics, superposition allows qubits to represent and process information in a more comprehensive and effective way. In classical systems, a bit can acquire only one of the two values at a given time; however, in quantum systems, the qubits exist in superposition of both the values at the same time until a measurement is taken. Thereafter, after performing measurement, the coherence (coherent superposition) is destroyed and the quantum system crumbles to one of the two states. A dual-level quantum system is represented by a qubit, which is a vector in two dimensions. The state vectors in quantum mechanics are represented by "Bra-ket" notation $|0\rangle$ and $|1\rangle$ and they are the linear superposition of two orthonormal bases

$$\begin{aligned}
|0\rangle &= \begin{pmatrix} 1 \\ 0 \end{pmatrix} \\
|1\rangle &= \begin{pmatrix} 0 \\ 1 \end{pmatrix}.
\end{aligned}
\tag{2.1}$$

Both of these orthonormal computational basis $|0\rangle$ and $|1\rangle$ are said to span the qubits in 2D hilbert space. In addition to it, we can make product basis states by combining qubit basis states and the collection of qubits at one place is known as "Quantum Register". Let's take an example, we can constitute 4D linear vectors space from qubits defined in above equation

$$\begin{aligned}
|0\rangle \otimes |0\rangle &= |00\rangle = \begin{bmatrix} 1 \\ 0 \\ 0 \\ 0 \end{bmatrix} \\
|0\rangle \otimes |1\rangle &= |01\rangle = \begin{bmatrix} 0 \\ 1 \\ 0 \\ 0 \end{bmatrix} \\
|1\rangle \otimes |0\rangle &= |10\rangle = \begin{bmatrix} 0 \\ 0 \\ 1 \\ 0 \end{bmatrix} \\
|1\rangle \otimes |1\rangle &= |11\rangle = \begin{bmatrix} 0 \\ 0 \\ 0 \\ 1 \end{bmatrix}.
\end{aligned}
\tag{2.2}$$

Generally we can also design n qubits by taking a superposition state vector that is present in 2^n dimensional space.

2.2 Quantum Systems

Quantum systems range from simpler (one particle) to complex (many particles) composite systems. A bipartite system composed of two qubits each having two computational basis. A bipartite system is an example of the most basic system that can be used to analyse entanglement [45]. Likewise, a tripartite system has three sub systems or qubits. Generally the state of a composite system (bipartite and tripartite) can be denoted as,

$$|\psi\rangle = \sum_{jk} c_{jk} |jk\rangle \quad (\text{BipartiteSystem}) \quad (2.3)$$

$$|\chi\rangle = \sum_{jkl} c_{jkl} |jkl\rangle \quad (\text{TripartiteSystem}). \quad (2.4)$$

Normalization requires $\sum_{jk} |c_{jk}|^2 = 1$ and $\sum_{jkl} |c_{jkl}|^2 = 1$. Thus, a separable bipartite pure state is a direct product of pure states in \mathcal{H}_A and \mathcal{H}_B

$$|\chi\rangle_{AB} = |\psi\rangle_A \otimes |\psi\rangle_B. \quad (2.5)$$

Multipartite systems consists of many qubits with individual basis vectors. The state of an N qubit system can be broadly described as

$$|n\rangle = |i_N\rangle \otimes |i_{N-1}\rangle \otimes \dots \otimes |i_1\rangle, \quad (2.6)$$

where $|ik\rangle \in [0, 1]$.

2.3 Density Operator

In quantum mechanics, density operator is represented by the Greek symbol ρ that expresses the state of the statistical ensemble. An ensemble is a statistical mixture of large number of particles/ subsystems with each subsystem as the possible state with

a certain probability that the system might acquire. For a quantum mechanical system undergoing measurement operations, exclusive state representation doesn't suffice, hence density matrix approach is used[46]. A projection of ket vectors accounts for the density matrix for pure states

$$\rho = |\phi\rangle\langle\phi|, \quad (2.7)$$

whereas for a mixed state, the density matrix is of the form

$$\rho = \sum_m P_m |\phi_m\rangle\langle\phi_m|. \quad (2.8)$$

The ket $|\phi_m\rangle$ are the number of states inherent in the statistical ensemble accompanied by their corresponding probabilities P_m . The density operator of the mixed state has a unity trace and satisfies the positivity condition:

$$\text{Tr}(\rho) = \sum_m P_m \text{Tr}(|\phi_m\rangle\langle\phi_m|) = \sum_m P_m = 1 \quad (2.9)$$

and

$$\langle\psi|\rho|\psi\rangle = \sum_m P_m \langle\psi|\phi_m\rangle\langle\phi_m|\psi\rangle = \sum_m P_m |\langle\psi|\phi_m\rangle|^2 \geq 0, \quad (2.10)$$

where $|\psi\rangle$ is an arbitrary state in the hilbert space. The density matrix formulation is significant given the fact that it can reflect the presence of interference in a system. If the off-diagonal terms of the matrix are zero, then the states are incoherent. On the contrary, presence of non-zero off diagonal terms portrays the interference/coherence in the state. In general, for density matrix of any state, the following three basic conditions must be fulfilled:

- For any state vector $|n\rangle$, the density matrix is a positive definite i.e.

$$\langle n|\rho|n\rangle \geq 0.$$

- The density matrix is idempotent i.e.

$$\rho^2 = \rho.$$

- The trace of a valid density matrix is always unity

$$\text{Tr}(\rho) = 1.$$

2.4 Categorization of States

In quantum mechanics, the wave vector associated with a system is a complete mathematical entity to probe into the behaviour of the system upon evolution and measurements. Quantum system is divided into two basic states i.e. pure and mixed and we discuss these states by using density operator.

2.4.1 Pure State

The quantum states which are solely represented mathematically by a wave vector $|\chi\rangle$ and graphically as a ray in complex hilbert space are called pure states. They can't be expressed in the convex combination of various other states, however are taken as linear combination of basis vectors/kets $|\chi\rangle = \sum_i a_i |j_i\rangle$. The density matrix of a pure state is

$$\rho = |\chi\rangle\langle\chi|. \quad (2.11)$$

Vectors of pure states occupy the sphere's surface in bloch sphere notation and possess norm 1. Density matrix serves as a pointer for the purity inherent in the states. If the ensemble is composed of pure states then trace over the squared density matrix equals one i.e., $\text{Tr}(\rho^2) = 1$.

2.4.2 Mixed State

Pure states in a statistical ensemble give rise to the mixed states. A single ket vector cannot be attributed to a mixed state rather they are defined by a density matrix of the form

$$\rho = \sum_s P_s |\chi_s\rangle\langle\chi_s|, \quad (2.12)$$

where,

$$\sum P_s = 1, \quad 0 < P_s \leq 1, \quad (2.13)$$

where P_s are the weighting factors/probabilities corresponding to the pure states $|\chi_s\rangle$ in the ensemble. For a given system, if the state is mixed then the trace of its squared density matrix is less than one i.e., $\text{Tr}(\rho^2) < 1$ [47].

2.5 Entanglement

The word entanglement means “state of being involved in complicated circumstances”. So, in quantum mechanics “quantum entanglement” is a complicated affair between two or more states or particles. The word “quantum entanglement” was first introduced by Erwin Schrödinger [48]. One of the key concepts, which distinguish quantum mechanics from the classical world is the quantum correlation between quantum states, and this interesting property has no classical analog. This concept was examined by Albert Einstein, Nathan Rosen, and Boris Podolsky (APR) [49] in their 1935 article that how correlated states would interact with each other, and they agreed that when two particles are deeply entangled, they destroy their own quantum state and can be regarded as one quantum state. Quantum entanglement is an important and counter-intuitive concept of quantum mechanics, which has deep connections with quantum information science [50]. The quantum correlated states are extensively employed for the tests of quantum mechanical concepts and have been widely researched in the areas of quantum communication [51], quantum computing [52], quantum cryptography [53], and quantum metrology [54].

2.5.1 Quantification of Entanglement

Given a composite system, the first question that flashes our mind is to what degree is the system entangled? In quantum entanglement theory, finding a satisfying answer to this question is the pivotal subject. Lately, a plethora of research is dedicated to this very issue. Since last few decades, there has been a tremendous work in the

area of quantum information and computation, the main gist of which revolves around entanglement. It is a useful resource and a valuable asset to this field. Knowing the fact that how much entanglement is intrinsic in a system is tantamount to the efficiency of that system to accomplish a desired task. Considering its significant role as a resource in information technology, multiple questions regarding its quantification arise such as to what extent the extraction of entanglement from quantum system is possible, for the preparation of system in a desired quantum state what degree of quantum entanglement is required and etc. An investigation on these frontiers is vital for error-free accomplishment of computational tasks. The investigation of composite systems is an integral component in quantum information and computation and variety of mathematical tools have been designed for this purpose such as density operators, Schmidt decomposition, von Neumann entropy etc.

Reduced von Neumann Entropy

One of the significant measures of entanglement is the reduced von Neumann entropy. Von Neumann entropy is the quantum extension of classical Shannon entropy. We describe the degree of entanglement of a system in terms of the difference of von Neumann entropies of its subsystems. Von Neumann entropy measures the quantum information of a state with density matrix ρ [55] and written as,

$$S(\rho) = -\text{Tr}(\rho \ln \rho) \tag{2.14}$$

which is expressed in terms of the eigenvalues as,

$$S(\rho) = -\sum_{k=1}^d \lambda_k \ln \lambda_k, \tag{2.15}$$

where λ_k are the singular values of the Schmidt decomposition or simply the non-zero eigenvalues of the matrix. For a pure state, the von Neumann entropy is zero which implies that upon identification once, no more additional information can be extracted from its copies. If a state is being transmitted between a sender and a receiver, then $S(\rho)$ is not the entropy at the end of the sender rather it quantifies the entropy of

the system that can be accessed by the receiver [56]. The entropy of the subsystems that make up the entire system is the reduced von Neumann entropy i.e. if we have a bipartite system which is the constitute of subsystems 1 and 2, then the reduced density matrix for one of the subsystems is attained by taking a partial trace over the other subsystem and likewise,

$$\rho_1 = \text{tr}_2(\rho) = \text{tr}_2(|\psi\rangle\langle\psi|). \quad (2.16)$$

The entropy of entanglement is stated mathematically as

$$E(\rho) = S(\rho_1) = S(\rho_2), \quad (2.17)$$

- Entropy of entanglement is zero $E = 0$ for the unentangled states.
- For entangled states $E > 0$.
- For states with maximal entanglement i.e., bell states $E = \log_2 d$ where d is the Hilbert space's dimension.

Since Schmidt decomposition is possible for only bipartite pure system so the entropy of entanglement is limited to bipartite pure systems only. When it comes to mixed states, the reduced Von Neumann entropy is no longer a reliable quantifier of entanglement because even in the absence of entanglement, each subsystem may show non-zero values for entropy. For such systems of mixed state, entanglement of formation, which will be touched upon briefly in the upcoming section, comes to the rescue.

Schmidt Decomposition

Quantum systems composed of subsystems that are interacting tend to become densely correlated losing their distinct individuality and become entangled. Schmidt decomposition is a useful tool to describe the entanglement and bring out the correlations between the subsystems using orthonormal bases. For a bipartite system of particles

α and β in pure state $|\chi\rangle$, there exists an orthonormal set of states $|\chi_k^\alpha\rangle$ and $|\chi_k^\beta\rangle$ for the subsystems α and β such that

$$|\lambda\rangle = \sum_k \lambda_k |\chi_k^\alpha\rangle |\chi_k^\beta\rangle, \quad (2.18)$$

where λ_k are non-negative real numbers obeying the normalization relation $\sum_k \lambda_k^2 = 1$. These expansion coefficients λ_k are the Schmidt's coefficients Schmidt decomposition. It expands the given vector into a set of special basis in such a way that all the expansion coefficients are real and there exists no cross-terms. For pure systems comprised of two particles, Schmidt decomposition serves as an excellent entanglement quantifier [57]. For the detection of entanglement, Schmidt coefficients λ_k play a significant role. To calculate these coefficients, we first construct the density matrix of the complete system, followed by a partial trace over one of the subsystems. For the state of the system $|\chi\rangle$, the density matrix is the outer product of the state vectors

$$\rho_{\text{sys}} = |\chi\rangle\langle\chi|. \quad (2.19)$$

Now take trace over one of the system, let's say β , we will extract the density matrix of the subsystem α as

$$\rho^{(\alpha)} = \text{Tr}_\beta |\chi\rangle\langle\chi|. \quad (2.20)$$

This reduced state is a diagonal matrix with $|\lambda_k|^2$ as the non-zero elements on the diagonal. The total number of strictly positive Schmidt coefficients of the state $|\chi\rangle$ counted with the multiplicity is defined as Schmidt rank or Schmidt number. They basically, are the pointers of entanglement in a two-particle system.

- For the state $|\chi\rangle$ to be separable, the Schmidt rank equals one. This indicates that the reduced density matrices $\rho^{(\alpha)}$ and $\rho^{(\beta)}$ of the subsystems are pure states and have only one strictly positive and non-zero eigenvalue.

- The state $|\chi\rangle$ is entangled if and only if it has a schmidt rank greater than one. This means that the reduced density matrices $\rho^{(\alpha)}$ and $\rho^{(\beta)}$ have more than one non-zero and positive eigenvalues and thus are mixed states.

2.6 Maximally Entangled State

The distinct quantum states of two qubits are maximally entangled states and they are called Bell States. There are four states in the superposition and linear combination of 0 and 1. These bell states are represented as

$$|\Phi^+\rangle = \frac{1}{\sqrt{2}} (|0\rangle_A \otimes |0\rangle_B + |1\rangle_A \otimes |1\rangle_B), \quad (2.21)$$

$$|\Phi^-\rangle = \frac{1}{\sqrt{2}} (|0\rangle_A \otimes |0\rangle_B - |1\rangle_A \otimes |1\rangle_B), \quad (2.22)$$

$$|\Psi^+\rangle = \frac{1}{\sqrt{2}} (|0\rangle_A \otimes |1\rangle_B + |1\rangle_A \otimes |0\rangle_B), \quad (2.23)$$

$$|\Psi^-\rangle = \frac{1}{\sqrt{2}} (|0\rangle_A \otimes |1\rangle_B - |1\rangle_A \otimes |0\rangle_B). \quad (2.24)$$

Alice's (subscript "A") qubit may be in a superposition of 0 and 1 with probability equal to 1/2 . If Bob (subscript "B") also measured her qubit in a superposition of 0 and 1, the result would be the same as for Alice if she uses the standard basis for measurements.

2.6.1 Generation Of Bell States

For instance, we have two coins (A and B) .There are four possible outcomes from those coins. Both can give head (H) or tail (T) at the same time or one can be head and other tail and vice versa. Lets say $|H\rangle$ corresponds to $|0\rangle$ and $|T\rangle$ corresponds to $|1\rangle$. A and B subscripts denotes the two coins and the possible outcomes of these two coins are given as

$$\begin{aligned}
|H\rangle_A|H\rangle_B &\longrightarrow |0\rangle_A|0\rangle_B, \\
|H\rangle_A|T\rangle_B &\longrightarrow |0\rangle_A|1\rangle_B, \\
|T\rangle_A|H\rangle_B &\longrightarrow |1\rangle_A|0\rangle_B, \\
|T\rangle_A|T\rangle_B &\longrightarrow |1\rangle_A|1\rangle_B.
\end{aligned}$$

To make first bell state 2.21, we take the first combination of coins in which both th coins are in head state and then apply Hadamard operator and CNOT operator. Hadamard operator is defined in its matrix form as

$$\hat{H} = \frac{1}{\sqrt{2}} \begin{pmatrix} 1 & 1 \\ 1 & -1 \end{pmatrix}. \quad (2.25)$$

First of all Hadamard operator is applied to create superposition state and after that CNOT operator is applied as shown below

$$\begin{aligned}
|0\rangle_A|0\rangle_B &\xrightarrow{\hat{H}} \left(\frac{|0\rangle_A + |1\rangle_A}{\sqrt{2}} \right) |0\rangle_B \\
&= \frac{|0\rangle_A|0\rangle_B + |1\rangle_A|0\rangle_B}{\sqrt{2}}
\end{aligned}$$

↓ CNOT

$$|\phi^+\rangle = \frac{1}{\sqrt{2}} (|0\rangle_A|0\rangle_B + |1\rangle_A|1\rangle_B).$$

The CNOT gate is a operation of two-qubits, in which the first qubit act as the control qubit and the second one as the target qubit. Lets say that the control qubit is $|1\rangle$ then the target qubit is flipped from state $|0\rangle$ to $|1\rangle$ and if the control qubit is $|0\rangle$ then the target qubit doesnt changes. Similarly by applying the same procedure (Hadamard followed by CNOT) on other coin combinations, we construct other bell states too (eq.2.22 to eq.2.24).

Chapter 3

Introduction to CRW and QW

3.1 Classical Random Walk(CRW)

Classical Random Walk (CRW) is the basic concept in both mathematics and physics as it gives a straightforward yet appropriate description for a variety of phenomenes. It explains the movement of a particle in discrete space and in all directions randomly so it is known as stochastic process. An experimental depiction of random walk is a Galton Board [58] which consists of multiple arrays of nails which are arranged such that when a ball slides down from top to bottom as shown in Fig 3.1, it's equally probable to move either to the left or right of the nail. Another example of the random walk such that motion of the particle on number line in classical manner in which its direction is chosen by the neutral (unbiased) coin. The particle moves towards the right direction if the coin comes up head and to the left direction if it comes up tail. This method is continually repeated. We cannot predict the particle positions at a subsequent time but instead we could determine the probability P at a point x at any time t . Initially, the particle is found at the origin at $(x=0, t=0)$, so the probability $P(t=0, x=0) = 1$. When particle is moved by one step, lets say $t=1$, it can be found at position $x=1$ or $x=-1$ with equal probability $1/2$, but now probability is zero at $x=0$. After doing this process again and again we can get the table 3.1. To calculate the expression of probability, lets assume that the number of forward steps is equals to 'a' and backward steps is equals to 'b'. When we add both a and b, we get the total number of steps 't'. Similarly, forward steps minus backward steps gives the position

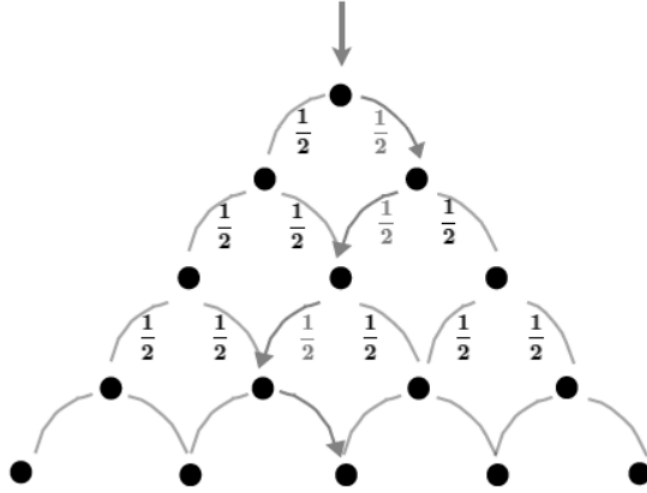


Figure 3.1: A classical Galton Board showing the multiple paths available for the particle.

of the particle 'x',

$$\begin{aligned} a + b &= t \\ a - b &= x. \end{aligned} \tag{3.1}$$

Now we can write forwards and backward steps in terms of x and t as follows,

$$\begin{aligned} a &= \frac{t+x}{2} \text{ (Forward steps)} \\ b &= \frac{t-x}{2} \text{ (Backward Steps)}. \end{aligned} \tag{3.2}$$

The probability of forward steps is calculated by utilizing the general probability formula,

$$\begin{aligned} p(t, x) &= \frac{1}{2^t} \binom{t}{a} \\ p(t, x) &= \frac{1}{2^t} \binom{t}{\frac{t+x}{2}}. \end{aligned} \tag{3.3}$$

Use Formula $\binom{a}{b} = \frac{a!}{(a-b)!b!}$ and then apply stirling approximation $x! \sim \sqrt{2\pi x} \left(\frac{x}{e}\right)^x$, we can get the probability expression as

$$p(t, x) = \frac{2}{\sqrt{2\pi t}} e^{-\frac{x^2}{2t}}. \tag{3.4}$$

t	-5	-4	-3	-2	-1	x=0	1	2	3	4	5
0						1					
1					$\frac{1}{2}$		$\frac{1}{2}$				
2				$\frac{1}{4}$		$\frac{1}{2}$		$\frac{1}{4}$			
3			$\frac{1}{8}$		3		$\frac{3}{8}$		$\frac{1}{8}$		
4		$\frac{1}{16}$		$\frac{1}{4}$		$\frac{3}{8}$		$\frac{1}{4}$		$\frac{1}{16}$	
5	$\frac{1}{32}$		32		$\frac{5}{16}$		$\frac{5}{16}$		$\frac{5}{32}$		$\frac{1}{32}$

Table 3.1: Probability distribution for a classical walk

This is clearly a Gaussian distribution that is used to represent a classical random walk. We can fix $t=100,200,500$ and then see the probabilities as shown in fig 3.2. Green coloured distribution is for $t=100$, orange for $t=200$ and blue for $t=500$. As the number of steps increases, we can get a wider range of possible positions, however, the distribution still remains centered around the mean position and decreases on both sides symmetrically and height of midpoint decreases when we increase number of steps. We can also calculate the envisaged distance from the origin. It is the distance of the particle from the origin as the number of steps are increasing. Statistically expected distance is the position standard deviation when we have symmetric probability distribution.

$$\sigma(t) = \frac{1}{\sqrt{2\pi t}} \int_{-\infty}^{\infty} x^2 e^{-\frac{x^2}{2t}} dx. \quad (3.5)$$

There are two inflection points in the normal distribution from the solutions of $\partial^2 p(t, x)/\partial x^2 = 0$ and the interval between the midpoint and its inflection point is defined as the standard deviation. In the next section, we will discuss the types of classical random walk- Discrete and Continuous Time Markov chains.

3.1.1 Discrete-time Markov Chain

Discrete-time Markov Chain (DTMC) take discrete values in a random manner and it must possess some properties i-e next states doesn't depend on the past state but it only depends on the current state and the next state is calculated by deterministic rules

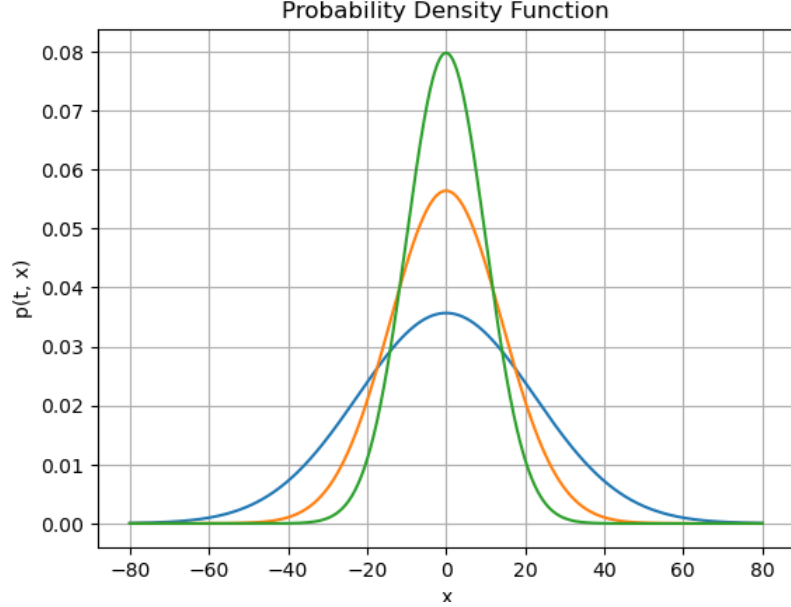


Figure 3.2: Probability distribution of a classical random walk

applied on the current state. The states and transitions between states in the Markov chain can be visualised as vertices and arcs, respectively, in a directed graph. The time of evolution maybe discrete or continuous but keep in mind that the set of states is always discrete. The context of discrete or continuous only pertains to time here. Let's describe the standard discrete-time Markov chain. The probability distribution is connected to each step in Markov Chain. First of all, select an order for the states and then the vector is used to represent the probability distribution. Lets assume a graph $\Gamma(V, X)$ having vertices $V = \{v_1, \dots, v_n\}$ ($|V| = n$) and edges X . Following vector is used to represent the probability distribution,

$$\begin{bmatrix} p_1(t) \\ \vdots \\ p_n(t) \end{bmatrix},$$

where $p_i(t)$ is the walker's probability at time t on vertex v_i . The action starts with the walker on the first vertex $v_1(0) = 1$ and $p_i(0) = 0$ for $i = 2 \dots n$. We cannot predict the walker's precise location after some time in a Markov chain but we may calculate the probability distribution if transition matrix T is given. T is also called

the stochastic matrix. If the distribution at time t is already known, we can acquire the probability distribution after some later time $t+1$ as

$$p_i(t+1) = \sum_{j=1}^n T_{ij} p_j(t). \quad (3.6)$$

In vector notation it is represented as,

$$\vec{p}(t+1) = T\vec{p}(t). \quad (3.7)$$

The Matrix T must follow some conditions: The entries of the matrix must be non-negative real numbers, and the sum of the entries in any column must be equal to one. The size of the matrix T is described by the state of the system that is being designed. Let's now turn our attention from the discrete-time classical random walk towards the idea of a continuous-time random walk.

3.1.2 Continuous-time Markov Chain

A Continuous-Time Markov Chain (CTMC) is a stochastic process that simulates a particle's movement in continuous time while giving arbitrary intervals of time between successive steps. The walker can move at any moment from vertex v_j to a neighbouring vertex v_i while time is a continuous variable. Contemplate the probability as if it were a liquid leaking from v_j to v_i to help you understand the dynamics. The walker is on vertex v_j in the start, and it will probably remain there for a short while. As the time passes, there are more chances of the walker to be found on adjacent vertices as the probability on v_j declines. Lets define a uniform transition rate given as β for all vertices and at all times. In order to solve for continuous variables, take infinitesimal time interval ϵ . The probability distribution of the Walker from the vertex v_j to vertex v_i is $\beta\epsilon$ and after sometime ϵ the probability on adjacent vertices is $k_j\beta\epsilon$. k_j is described as the degree of the vertex v_j has k_j adjacent vertices. $1-k_j\beta\epsilon$ is the probability of being at vertex v_j . The probability on vertex v_j , moving to vertex v_i during the time interval t is described by the $T_{ij}(t)$ of the transition matrix at time t in the continuous-time case.

$$T_{ij}(\epsilon) = \begin{cases} 1 - k_j\beta\epsilon + O(\epsilon^2), & \text{if } i = j; \\ \beta\epsilon + O(\epsilon^2), & \text{if } i \neq j. \end{cases} \quad (3.8)$$

Take an auxiliary matrix as ,

$$H_{ij} = \begin{cases} k_j\beta, & \text{if } i = j; \\ -\beta, & \text{if } i \neq j \text{ and adjacent}; \\ 0, & \text{if } i \neq j \text{ and non-adjacent}. \end{cases} \quad (3.9)$$

It is obvious that the probability of two independent events is the product of probability of each event so at different times we can multiply the transition matrices as,

$$T_{ij}(t + \epsilon) = \sum_l T_{il}(t)T_{lj}(\epsilon). \quad (3.10)$$

The index l runs on all the vertices and it runs on the vertices that are adjacent to v_j . Note that, if no edge is linking v_j and v_l , then $T_{lj}(\epsilon) = 0$. Now isolate $l = j$ and from eq. 3.8 and 3.9, we get

$$\begin{aligned} T_{ij}(t + \epsilon) &= T_{ij}(t)T_{jj}(\epsilon) + \sum_{l \neq j} T_{il}(t)T_{lj}(\epsilon) \\ &= T_{ij}(t) (1 - \epsilon H_{jj}) - \epsilon \sum_{l \neq j} T_{il}(t)H_{lj}. \end{aligned} \quad (3.11)$$

By rearranging the above equation, we get the differential equation as

$$\frac{dT_{ij}(t)}{dt} = - \sum_i H_{ij}T_{il}(t). \quad (3.12)$$

Use the initial Condition $T_{ij}(0) = \delta_{ij}$, the solution of differential equation is

$$T(t) = e^{-Ht}. \quad (3.13)$$

Exponential functions can be easily expanded by the Taylor Series, lets say our initial distribution is denoted by $\vec{p}(0)$ then we get

$$\vec{p}(t) = T(t)\vec{p}(0). \quad (3.14)$$

See the resemblance with eq. 3.7, in this way it is compared with discrete case [59]. Random walks have several applications in various fields, such as physics, biology, computer science, social sciences, image and signal processing, and more. They are used to describe the behavior of polymers and the diffusion of particles in fluids to model the movement of molecules and atoms and to study the behaviour of complex systems and phase transitions etc.

3.1.3 Limitations of Classical Random Walk

Apart from the fact that classical random walk performs an important role in many domains of physics but it has some limitations. In classical random walk there is a localization of particles over time i.e., they tend towards the initial position. Also there are no interference effects in classical random walk. Entanglement is also missing in classical random walk which can give solutions to non trivial correlations between distant positions. So we are moving towards the quantum walk that contains more spread (over a large area) at different positions as compared to classical walk and also contains probability amplitudes for different parts creating interference patterns either constructively or destructively heading to amplification or suppression at specific positions. Entanglement is another important thing that is present in Quantum walk, for example the entanglement between found in the position of the particle and other degrees of freedom such as its spin. Quantum entanglement is also very important in constructing complex quantum algorithms and protocols [60]. So, in following section, quantum walk is discussed in detail.

3.2 Quantum Walk (QW)

The quantum mechanical counterpart of the classical random walk is a quantum walk in which the probability amplitudes are transformed by the unitary transformations that incorporates the interesting interference effects rather than the probabilities by stochastic matrix as in classical random walk [21]. Typically, a procedure known as quantization is used to develop quantum models along with their equations. Energy

and Momentum of classical are changed by the operators in quantum mechanics that perform action on a Hilbert space. The degrees of freedom of the system decides the size of these operators. A quantum state is characterised by a vector in the Hilbert space and its evolution is guided by a unitary operation if it is completely isolated from the interactions with the macroscopic world around it. If the system consist of two or more than two components, then the total Hilbert Space consists of the tensor product of the Hilbert space of all the components. Quantum walk models are used to frame different quantum algorithms and information processing [9]. Likewise Classical Walk, Quantum walk are also segregated into two types - discrete and continuous and the coined quantum walk is a type of discrete quantum walk.

3.2.1 Discrete Time Quantum Walk

Discrete time Quantum walk Model (DTQWM) was first discussed by Aharonov et al [61] in 1993 and it is the mostly used model of quantum computation. It is applied on discrete positions in discrete steps. Coined Quantum walk is also included in discrete time Quantum walk. It will be explained in detail later on. In order to find the state after some steps, unitary operator U is applied on the initial state and as a result we got the final state. Lets say ϕ_1 is initial state and ϕ_2 is final state,

$$|\phi\rangle_2 = \hat{U}|\phi\rangle_1. \tag{3.15}$$

3.2.2 Continuous Time Quantum Walk

Continuous Quantum walk was proposed by Farhi and Guttman [62]. The evolution operator in this type of work is the Hamiltonian (H) of the system. The walker's position is evolved by applying the operator at any time(t). As the name suggests, the walk is continuous having no restrictions on time and the walker evolves by application of the operator at any time (t). Mathematically, the evolution in this model is governed by the Schrodinger equation,

$$|\phi\rangle_t = \exp(-iHt)|\phi\rangle_1. \tag{3.16}$$

3.3 Coined Quantum Walk on a line

Discrete time coined quantum walk is also known as coined model. As an example we took a one dimensional lattice on a line. The position of the Walker is evolved by a Quantum "coin". In quantum mechanic case, the position of the Walker "z" is taken as a vector $|z\rangle$. First of all , if the result is head then the next position will be $|z + 1\rangle$ and if it is tail then the next position is $|z - 1\rangle$. For example, our walker is an electron and its state is determined by the position as well as the value of the spin i.e. up, down. The direction of the motion is described by the spin of the electron for example it goes to $|z + 1\rangle$ if the spin is up and it goes to $|z - 1\rangle$ if it is down.

The total Hilbert space of the system \mathcal{H}_{total} is described by the Kronecker product of the Hilbert spaces of both, the coin \mathcal{H}_{coin} and the position \mathcal{H}_{pos} of the particle.

$$\mathcal{H}_{total} = \mathcal{H}_{coin} \otimes \mathcal{H}_{pos}. \quad (3.17)$$

Imagine the particle is spotted at the position $|pos\rangle$ and the coin state $|coin\rangle$

$$|\phi(initial)\rangle = |pos\rangle|coin\rangle. \quad (3.18)$$

Lets say the particle's initial position is zero.

$$|\phi(0)\rangle = |0\rangle|coin\rangle, \quad (3.19)$$

The coin States can be spin up and down, $|\uparrow\rangle = \begin{pmatrix} 1 \\ 0 \end{pmatrix}$ and $|\downarrow\rangle = \begin{pmatrix} 0 \\ 1 \end{pmatrix}$. These states will be explained in more detail in the next section. The state after evolution of N steps,

$$|\phi(N)\rangle = V^N|\phi(0)\rangle. \quad (3.20)$$

Following is the unitary operator that is used to illustrate the dynamics of the quantum walk

$$Unitary(\hat{V}) = Shift(\hat{S})[coin(\hat{C}) \otimes Identity(\hat{I}_p)]. \quad (3.21)$$

First of all, the operator $\hat{C} \otimes \hat{I}_p$ is applied to the initial state $|\phi(initial)\rangle$. Here \hat{I}_p is described as the identity operator of the position Hilbert space \mathcal{H}_{pos} . The operator \hat{C} is applied to the coin state but the walker's position (denoted as 'z') remains at the same position. The shift of the Walker is carried out by the shift operator as

$$\hat{S} = \sum_z (|z-1\rangle\langle z|) \otimes |\downarrow\rangle\langle\downarrow| + \sum_z (|z+1\rangle\langle z|) \otimes |\uparrow\rangle\langle\uparrow|. \quad (3.22)$$

The action of the shift operator is as follows

$$\begin{aligned} S|\uparrow\rangle|z\rangle &= |\uparrow\rangle|z+1\rangle \\ S|\downarrow\rangle|z\rangle &= |\downarrow\rangle|z-1\rangle. \end{aligned} \quad (3.23)$$

Hadamard coin is the mostly used quantum coin its matrix form is

$$\hat{C} = \hat{H} = \frac{1}{\sqrt{2}} \begin{pmatrix} 1 & 1 \\ 1 & -1 \end{pmatrix}. \quad (3.24)$$

Hadamard gives the 50:50 superposition when applied on the state as shown below

$$\begin{aligned} \hat{H}|\uparrow\rangle &= \frac{1}{\sqrt{2}}(|\uparrow\rangle + |\downarrow\rangle) \\ \hat{H}|\downarrow\rangle &= \frac{1}{\sqrt{2}}(|\uparrow\rangle - |\downarrow\rangle). \end{aligned} \quad (3.25)$$

Hadamard is only applied to the coin state but at that time the position of the walker remains the same, then shift operator is applied to shift the walker. Now moving further, different coin states are taken and their dynamics in quantum walk is studied and the result shows that how the probabilities will change when different coin states are used but keeping the initial position state of the particle at zero on the number line.

3.3.1 Spin-up Coin State :

Lets say the initial state eq.3.19 in spin up state of the coin will become

$$|\phi_{ini}(0)\rangle = |0\rangle_p |\uparrow\rangle_c. \quad (3.26)$$

Apply unitary operator,

$$|\phi_1 \rangle = \hat{V} |\phi_{ini} \rangle = \frac{1}{\sqrt{2}}(|-1, \downarrow\rangle + |+1, \uparrow\rangle). \quad (3.27)$$

As it can be seen clearly that there is equal probability at position 1 and -1. The unbiased Hadamard coin is used such that the probability that goes to left and right is equal. Classically, the particle would be present at one of the positions either 1 or -1. However when measurements are performed the system would collapse into 1 or -1 with equal probability which is similar to the classical results. Lets move ahead and take more steps. After second step,

$$\hat{V}\hat{V} |\phi_{ini}\rangle = \hat{V}^2 |\phi_{ini}\rangle = \frac{1}{2}(|2, \uparrow\rangle + |0, \downarrow\rangle + |0, \uparrow\rangle - |-2, \downarrow\rangle). \quad (3.28)$$

After third step,

$$\hat{V}\hat{V}\hat{V} |\phi_{ini}\rangle = \hat{V}^3 |\phi_{ini}\rangle = \frac{1}{2\sqrt{2}}(|3, \uparrow\rangle + |1, \downarrow\rangle + 2|1, \uparrow\rangle - |-1, \uparrow\rangle + |-3, \downarrow\rangle). \quad (3.29)$$

The ultimate state after "N" steps of the particle will be calculated as

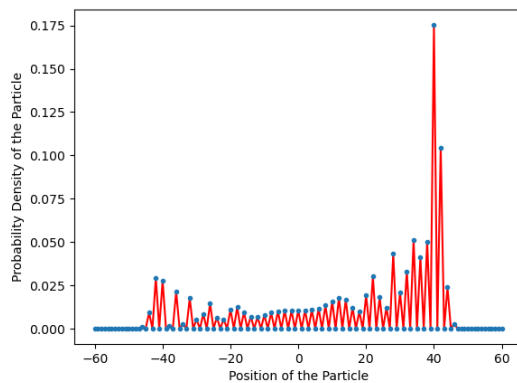
$$V^N |\phi_{ini}\rangle = \sum_{j=-N}^{+N} (a_{\uparrow}(j) |j, \uparrow\rangle + a_{\downarrow}(j) |j, \downarrow\rangle), \quad (3.30)$$

where $a_{\uparrow}(j)$ and $a_{\downarrow}(j)$ are the probability amplitudes in up and down coin state of the particle at position j , respectively. Hence its unitary, so the summation of probabilities should be equal to one,

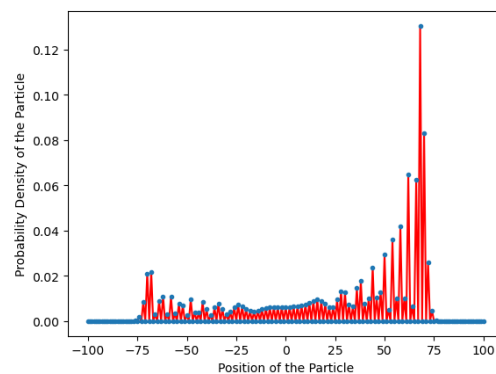
$$\sum_{j=-N}^N |a_{\uparrow}(j)|^2 + |a_{\downarrow}(j)|^2 = 1. \quad (3.31)$$

The expectation value of the coin state projector onto the position l with the final state gives the total likelihood of finding the walker at position l after N steps is

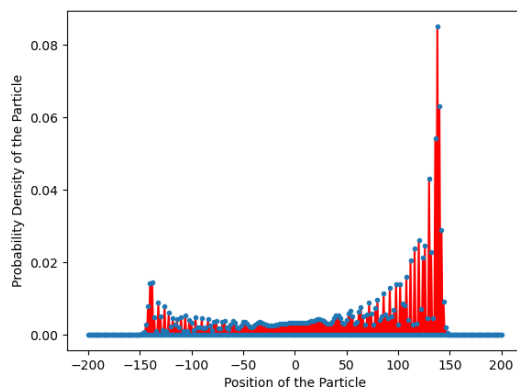
$$P(l) = \langle \phi_{fin} | l \rangle \langle l | \otimes (| \uparrow \rangle \langle \uparrow | + | \downarrow \rangle \langle \downarrow |) | \phi_{fin} \rangle, \quad (3.32)$$



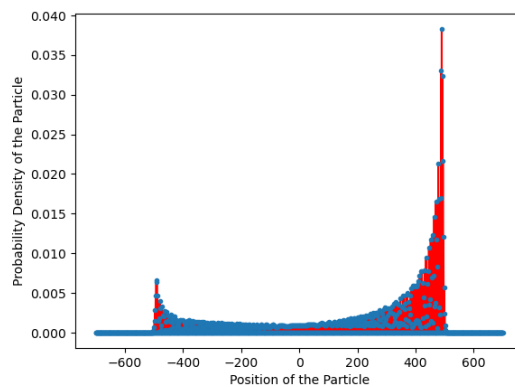
(a) $N=60$



(b) $N=100$



(c) $N=200$



(d) $N=700$

Figure 3.3: The probabilities of the walker after 60,100,200,700 steps of the walk with a coin in the up spin state are plotted against the positions where the walker can be located. The right going amplitudes undergo constructive interference hence enhancing the probabilities towards the right side on the line.

$$P(l) = \langle \phi_{\text{fin}} | l \rangle \langle l | \otimes | \uparrow \rangle \langle \uparrow | \phi_{\text{fin}} \rangle + \langle \phi_{\text{fin}} | l \rangle \langle l | \otimes | \downarrow \rangle \langle \downarrow | \phi_{\text{fin}} \rangle, \quad (3.33)$$

$$P(l) = |a_{\uparrow}(l)|^2 + |a_{\downarrow}(l)|^2. \quad (3.34)$$

Evaluating and comparing the probabilities after different number of steps, we see a marked difference between the probabilities of classical walk to those of quantum walk. For the first two steps, the distribution is alike, however, as the quantum walk progresses, its probability distribution deviates from classical counterpart due to interference. Following a walk for 60,100,200 and 700 steps, the probability distribution of the walker is plotted against the position showing the walk is more inclined towards the right if the initial spin state of the coin is up. In other words, for the walker starting up in up coin state, more right transitioning amplitudes interfere constructively than the left-transitioning amplitudes, thus forming a peak on the right side. As the number of steps are increasing, the particles move away from the mean position. Now we ll take spin down as a initial coin state and will observe the behaviour of the walker.

3.3.2 Spin-Down Coin State :

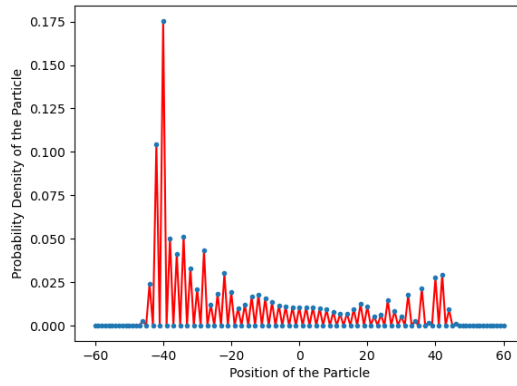
Lets say the initial state eq.3.19 in spin down state of the coin will become

$$|\phi_{\text{ini}}(0)\rangle = |0\rangle_p | \downarrow \rangle_c. \quad (3.35)$$

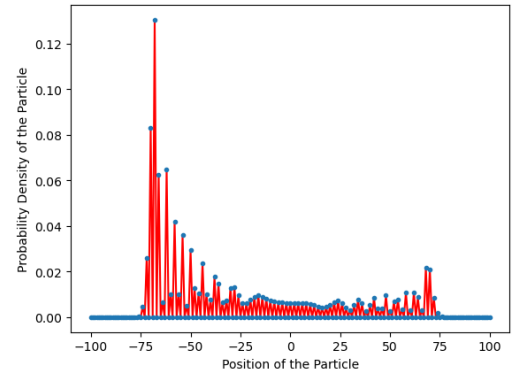
Applying unitary operator,

$$|\phi_1 \rangle = \hat{V} |\phi_{\text{ini}} \rangle = \frac{1}{\sqrt{2}}(|1, \uparrow \rangle + | -1, \downarrow \rangle). \quad (3.36)$$

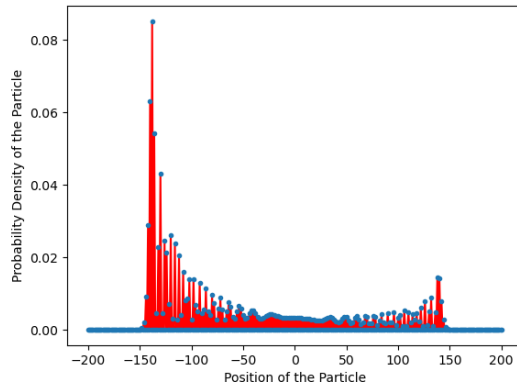
As it can be seen clearly that there is equal probability at position 1 and -1. The unbiased hadamard coin is used such that the probability goes to left and right is equal. Classically, the particle would be present at one of the positions either 1 or -1. However when measurements are performed, the system would collapse into 1 or -1 with equal



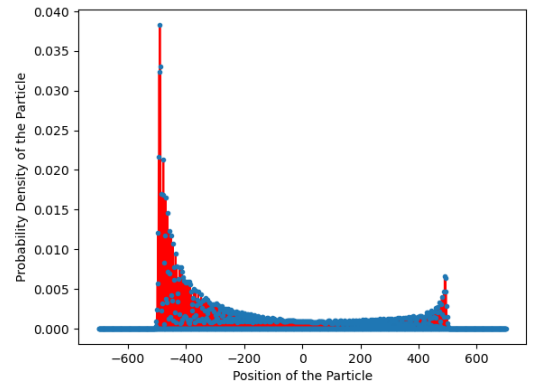
(a) $N=60$



(b) $N=100$



(c) $N=200$



(d) $N=700$

Figure 3.4: The probabilities of the walker after 60,100,200,700 steps of the walk with a coin in the down spin state are plotted against the positions where the walker can be located. The left going amplitudes undergo destructive interference hence enhancing the probabilities towards the left side on the line.

probability that is similar to the classical results. Lets move ahead and take more steps. Again apply unitary operator to see the walker's position after second step,

$$\hat{V}\hat{V}|\phi_{ini}\rangle = \hat{V}^2|\phi_{ini}\rangle = \frac{1}{2}(|2, \uparrow\rangle + |0, \downarrow\rangle - |0, \uparrow\rangle + |-2, \downarrow\rangle). \quad (3.37)$$

After third step,

$$\hat{V}\hat{V}\hat{V}|\phi_{ini}\rangle = \hat{V}^3|\phi_{ini}\rangle = \frac{1}{2\sqrt{2}}(|3, \uparrow\rangle + |1, \downarrow\rangle - 2|-1, \downarrow\rangle + |-1, \uparrow\rangle - |-3, \downarrow\rangle). \quad (3.38)$$

In a similar fashion, the walker continues to take steps and rest of the states can be computed. After three steps, it's observed that the probability of the particle to acquire position +1 decreases because of destructive interference whereas constructive interference makes the particle more likely to occupy position -1. In the example of classical random walk, the probability distribution shows a binomial trend and centers at the origin i.e. the beginning point of the walker. Contrary, during investigation of the quantum walk of 60, 100, 200 and 700 steps for the above initial state, the graph peaks at -45, -70, -140 and -500 position, respectively. This asymmetric behaviour of the probability distribution is attributed to interference, the coin operator, the coin states and their superposition. At the third step, the probability of the walker to be found at position 1 and -1 in CRW is 3/8 each whereas in QW, the walker is more probable to be at position -1 as compared to +1. This is because the destructive interference causes decline in the probability for transmission to +1 position; on the other hand, constructive interference decreases the likelihood of the walker at -1 position. In short, for the walker with down coin state, more left-transitioning amplitudes interfere constructively than the right-transitioning amplitudes, thus forming a peak on the left side.

3.3.3 Superposition Coin State :

In the previous subsections, we acquired different probability distributions just by shifting the state of the coin and keeping the starting position of the walker same. Now, we are interested in finding out the effect on probabilities given the coin state is a symmetric superposition of up and down coin states. Let the initial state be

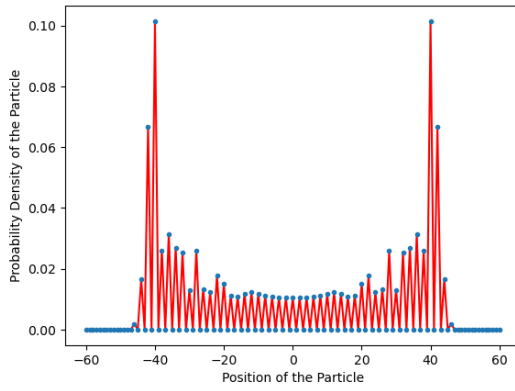
$$|\phi_{ini}\rangle = |0\rangle_p \otimes \frac{1}{\sqrt{2}}(|\uparrow\rangle + i|\downarrow\rangle)_c. \quad (3.39)$$

Applying the Hadamard and the shift operator step by step, the walker progresses on the line. The states of the walker after two steps are:

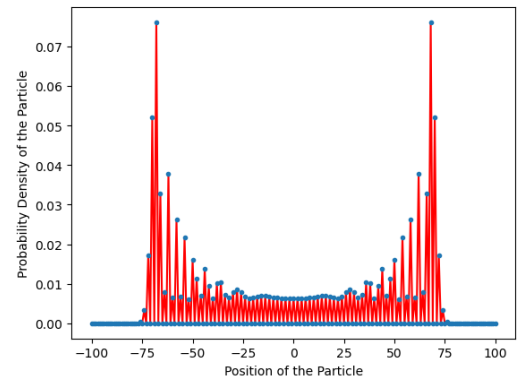
$$\hat{V} |\Phi_{ini}\rangle = \frac{1}{2}[|\uparrow, 1\rangle + |\downarrow, -1\rangle + i|\uparrow, 1\rangle - |\downarrow, -1\rangle], \quad (3.40)$$

$$\begin{aligned} \hat{V}^2 |\phi_{ini}\rangle = \frac{1}{2\sqrt{2}}[&|\uparrow, 2\rangle + |\downarrow, 0\rangle + |\uparrow, 0\rangle \\ &- |\downarrow, -2\rangle + i|\uparrow, 2\rangle + i|\downarrow, 0\rangle \\ &- |\uparrow, 0\rangle + i|\downarrow, -2\rangle]. \end{aligned} \quad (3.41)$$

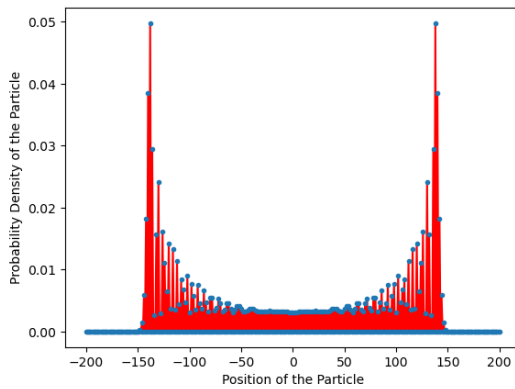
For symmetric initial state of the walker, there is a symmetry in the probability distribution. When unitary is applied, terms containing the unreal(imaginary) units are not replaced into the terms not having the imaginary units, and vice versa. The terms of the walk, that turns to the right are not cancelled by the left-moving terms of the quantum walk. The probability distributions are always added at the end. The walker with superposition coin state, the left-transitioning amplitudes are equal to the right-transitioning amplitudes, thus forming a peaks on the both sides as shown in fig 3.5. The quantum walk of 60, 100, 200 and 700 steps for the superposition coin state gives the extreme probability peaks at 0.10, 0.08, 0.05 and 0.025, respectively. This symmetric behaviour of the probability distribution is attributed to equal constructive and destructive interferences, the coin operator, the coin states and their superposition.



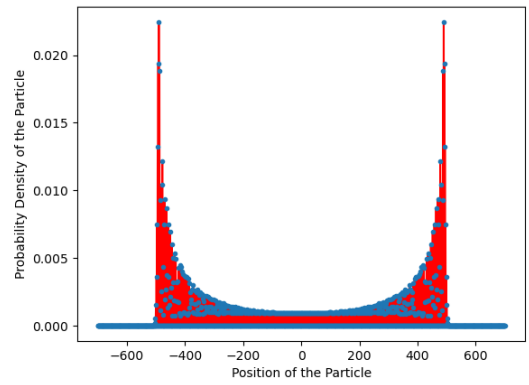
(a) $N=60$



(b) $N=100$



(c) $N=200$



(d) $N=700$

Figure 3.5: The probabilities of the walker after 60, 100, 200 and 700 steps of the walk with a coin in the superposed spin state are plotted against the positions where the walker can be located.

From the experimental results, it is quite evident that the CRW always follows binomial probability distribution regardless of the initial state of the walker whereas the quantum walk is highly dependent on the walker's initial state. The "mother" distribution from which the other two distributions can be derived, the binomial distribution describes the number of positive results in experiments. The Gaussian distribution can be thought of as a particular case of the binomial distribution and it is applicable to a wide range of variables.

In the next chapter, we will discuss the quantum walk with coin states having different values of entanglement for example, separable coin state (zero entanglement), partially entangled coin and maximally entangled state. The results for these states are explained in detail.

Chapter 4

Quantum Walk with Bipartite Entangled Coins

In this chapter we will analyze quantum walk with bipartite coin states i.e. separable, partially entangled and maximally entangled state. By using these different coin states, we observe several types of probability distributions. Lets begin this chapter with distribution of quantum walk with separable coin state.

4.1 Quantum Walk with Separable Coin State

Quantum states that may be factored into independent states that correspond to different subspaces are known as separable states. For instance, we take separable coin (sc) and initialize the coin state as,

$$|\text{coin}\rangle_{sc} = \frac{1}{2}(|0\rangle + |1\rangle)_c(|0\rangle + |1\rangle)_c. \quad (4.1)$$

The particle is at origin so $|\text{pos}\rangle = |0\rangle_p$, so the initial state (from eq.3.19) of the composite system would become,

$$|\phi(\text{initial})\rangle_{sc} = |0\rangle_p \otimes \frac{1}{2}(|0\rangle + |1\rangle)_c(|0\rangle + |1\rangle)_c, \quad (4.2)$$

The Hilbert space of the composite system is the tensor product of the position Hilbert space and separable coin (sc) Hilbert space

$$\mathcal{H}_{sys} = \mathcal{H}_p \otimes \mathcal{H}_{sc}. \quad (4.3)$$

As a coin evolution operator, we employed the Hadamard operator in the simplest case of the quantum walk with a single coin. In ket-bra notation, the Hadamard can be written in the form as,

$$\hat{H} = \frac{1}{\sqrt{2}}(|0\rangle\langle 0| + |0\rangle\langle 1| + |1\rangle\langle 0| - |1\rangle\langle 1|), \quad (4.4)$$

Now that our coin state comprises of a bipartite system, we devise its coin operator by taking tensor product over the single coin evolution operators,

$$\hat{G} = \hat{H} \otimes \hat{H}, \quad (4.5)$$

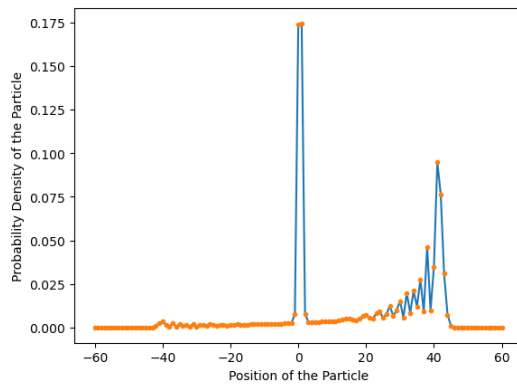
so,

$$\begin{aligned} \hat{G} = \frac{1}{2} & (|00\rangle\langle 00| + |01\rangle\langle 00| + |10\rangle\langle 00| + |11\rangle\langle 00| \\ & + |00\rangle\langle 01| - |01\rangle\langle 01| + |10\rangle\langle 01| - |11\rangle\langle 01| \\ & + |00\rangle\langle 10| + |01\rangle\langle 10| - |10\rangle\langle 10| - |11\rangle\langle 10| \\ & + |00\rangle\langle 11| - |01\rangle\langle 11| - |10\rangle\langle 11| + |11\rangle\langle 11|). \end{aligned} \quad (4.6)$$

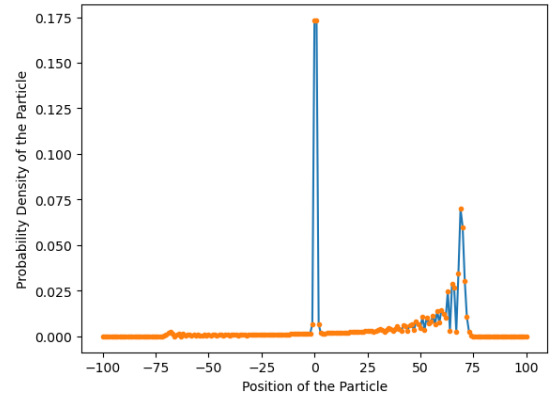
The shift operator comes before the coin operator, and it uses the walker's position (z) state to determine whether to advance it to the right or left by one step. It is given as under

$$\begin{aligned} \hat{S} = & |00\rangle\langle 00| \otimes \sum_z |z+1\rangle\langle z| + |01\rangle\langle 01| \otimes \sum_z |z\rangle\langle z| \\ & + |10\rangle\langle 10| \otimes \sum_z |z\rangle\langle z| + |11\rangle\langle 11| \otimes \sum_z |z-1\rangle\langle z|. \end{aligned} \quad (4.7)$$

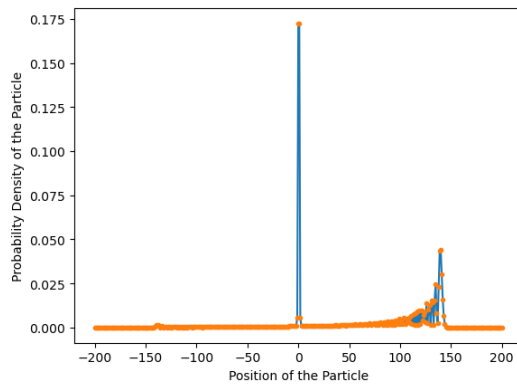
This shift operator specifies the transformation rules for the position of the particle in a Quantum walk. When the state of the coin is $|00\rangle$ and $|11\rangle$, then the particle position is incremented by 1 and decremented by 1, respectively. While the position



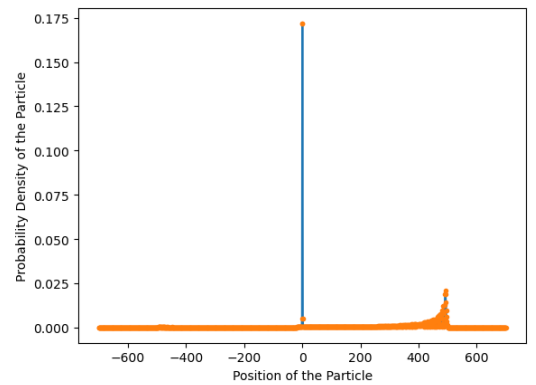
(a) $N=60$



(b) $N=100$



(c) $N=200$



(d) $N=700$

Figure 4.1: Probabilities for locating the walker at various positions after 60, 100, 200 and 700 steps of the walk using a separable coin state. It reproduces a similar graph as that of spin-up coin state. It shows that the use of separable state with real coefficients distributes the probability to only one side of the graph.

remains unchanged when the state of the coin is $|01\rangle$ and $|10\rangle$. The combined evolution operator of the system is

$$V_{sc} = \hat{S} \cdot (\hat{G} \otimes I_p). \quad (4.8)$$

Again apply unitary operator to see the walker's position after first step,

$$|\phi(1)\rangle = V|\phi\rangle_{\text{initial}} = |1\rangle_p |00\rangle_c. \quad (4.9)$$

After second step,

$$|\phi(2)\rangle = V^2|\phi\rangle_{\text{initial}} = \frac{1}{2} (|2\rangle_p |00\rangle_c + |1\rangle_p |01\rangle_c + |1\rangle_p |10\rangle_c + |0\rangle_p |11\rangle_c). \quad (4.10)$$

The state of the system after some steps N of the walk is given as

$$|\phi(N)\rangle = V_{sc}^N |\phi(\text{initial})\rangle_{sc}. \quad (4.11)$$

Applying the measurement operator onto the position states $|k\rangle$, we can compute the probability of existence of the walker on these positions. Measurement operator has the form

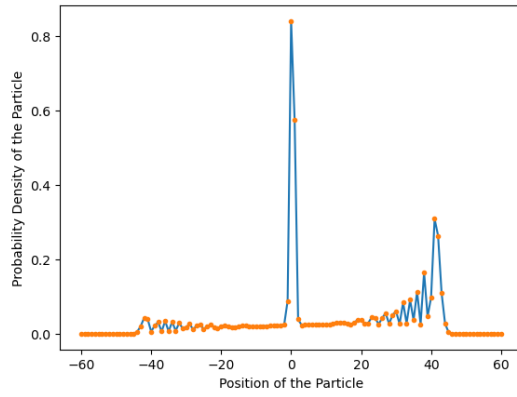
$$\hat{M}_p = \sum_k b_k |k\rangle_{pp} \langle k|. \quad (4.12)$$

For the coin state to be separable, the graph exhibits asymmetry (fig.4.1) or skewness towards the right which means that the particle approaches only the positions onto the right hand side of the origin.

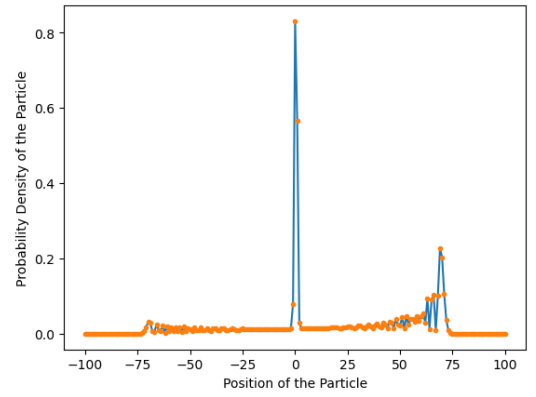
4.2 Quantum Walk with Partially Entangled Coin

We have already seen the behaviour of quantum walk by using separable coin state, let us now discuss it with the partially entangled coin (pec) as

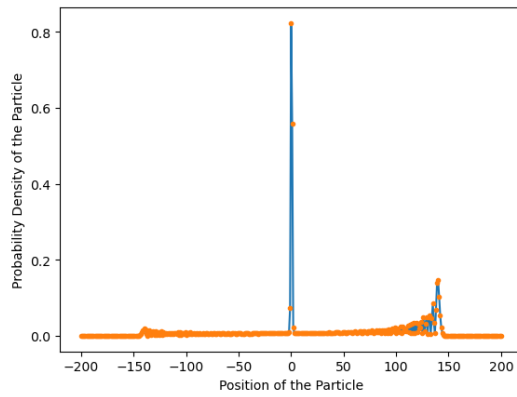
$$|\text{coin}\rangle_{pec} = \frac{1}{2}|00\rangle + \frac{1+\sqrt{3}}{4}|01\rangle + \frac{\sqrt{3}-1}{4}|10\rangle + \frac{1}{2}|11\rangle. \quad (4.13)$$



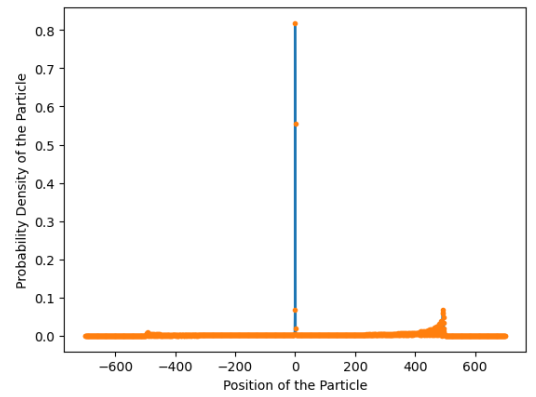
(a) $N=60$



(b) $N=100$



(c) $N=200$



(d) $N=700$

Figure 4.2: Probabilities for locating the walker at various positions after 60, 100, 200 and 700 steps of the walk using a partially entangled coin state.

The overall state of the Walker and coin system is,

$$|\phi(initial)\rangle_{pec} = |0\rangle_p \otimes \left[\frac{1}{2}|00\rangle + \frac{1+\sqrt{3}}{4}|01\rangle + \frac{\sqrt{3}-1}{4}|10\rangle + \frac{1}{2}|11\rangle \right]_c. \quad (4.14)$$

The system's evolution is directed by the following operator,

$$V_{pec} = S.(\hat{G} \otimes I_p), \quad (4.15)$$

where \hat{G} and \hat{S} are taken from eq.4.6 and eq.4.7, respectively. Assuming the walk for a N steps with the operation as,

$$|\phi(N)\rangle = V_{pec}^N |\phi(initial)\rangle_{pec}. \quad (4.16)$$

We have plotted the probability of locating the walker at various positions. Given that we have applied the same coin and shift operators in the above discussed case, we can easily tell the effect of partial entanglement on the quantum walk's probability distribution for different number of steps 60, 100, 200 and 700 as shown in figure 4.2. We can see that the peak on left hand side is slightly higher in the case of partially entangled coin as compared to separable coin state (where there is only a small hem on left hand side). Note that all the operators are same in both the cases. In our next section, we will see the walker's behaviour with maximally entangled coin in detail.

4.3 Quantum Walk with Maximally Entangled Coins

We will now examine the mathematical makeup of a quantum walk on a line with maximally entangled coin and a single walker in order to build a model for unrestricted quantum walks. A bipartite system with two entangled qubits serve as a coin. For maximal entanglement, bell states(eq.2.21-eq.2.24) are employed as coin states. Initially, the first bell state is considered as a coin state. From eq3.18, the particle is at position 0 on a number line and coin state to be taken as,

$$|\phi(initial)\rangle_{ec} = |0\rangle_p \otimes \left(\frac{|00\rangle + |11\rangle}{\sqrt{2}} \right)_c. \quad (4.17)$$

The evolution operator of the system we use is,

$$V_{ec} = \hat{S} \cdot (\hat{G} \otimes I_p). \quad (4.18)$$

where \hat{G} and \hat{S} are taken from eq.4.6 and eq.4.7, respectively. We observe the walk for first three steps. After first step,

$$|\phi^{(1)}\rangle = \frac{|0_c, 0_c, 1_p\rangle}{\sqrt{2}} + \frac{|1_c, 1_c, (-1)_p\rangle}{\sqrt{2}}. \quad (4.19)$$

After second Step,

$$\begin{aligned} |\phi^{(2)}\rangle &= \frac{|0_c, 0_c, 0_p\rangle}{2\sqrt{2}} + \frac{|0_c, 0_c, 2_p\rangle}{2\sqrt{2}} - \frac{|0_c, 1_c, (-1)_p\rangle}{2\sqrt{2}} \\ &+ \frac{|0_c, 1_c, 1_p\rangle}{2\sqrt{2}} - \frac{|1_c, 0_c, (-1)_p\rangle}{2\sqrt{2}} + \frac{|1_c, 0_c, 1_p\rangle}{2\sqrt{2}} \\ &+ \frac{|1_c, 1_c, (-2)_p\rangle}{2\sqrt{2}} + \frac{|1_c, 1_c, 0_p\rangle}{2\sqrt{2}}. \end{aligned} \quad (4.20)$$

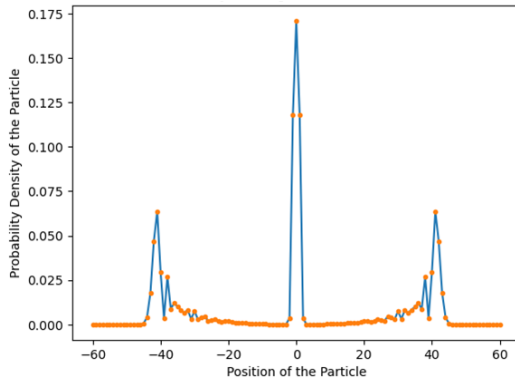
After third step,

$$\begin{aligned} |\phi^{(3)}\rangle &= \frac{|0_c, 0_c, (-1)_p\rangle}{4\sqrt{2}} - \frac{|0_c, 0_c, 0_p\rangle}{2\sqrt{2}} + \frac{|0_c, 0_c, 1_p\rangle}{2\sqrt{2}} \\ &+ \frac{|0_c, 0_c, 2_p\rangle}{2\sqrt{2}} + \frac{|0_c, 0_c, 3_p\rangle}{4\sqrt{2}} - \frac{|0_c, 1_c, (-2)_p\rangle}{4\sqrt{2}} \\ &+ \frac{(0_{c \leq 1_{cc} 2_p})}{4\sqrt{2}} - \frac{(1_{cc} 0_c (-2)_p)}{4\sqrt{2}} + \frac{(1_{cs} 0_c 2_p)}{4\sqrt{2}} \\ &+ \frac{|1_c, 1_c, (-3)_p\rangle}{4\sqrt{2}} + \frac{|1_c, 1_c, (-2)_p\rangle}{2\sqrt{2}} + \frac{|1_c, 1_{cc}, (-1)_p\rangle}{2\sqrt{2}} \\ &- \frac{(1_{c, 1, 0_p})}{2\sqrt{2}} + \frac{(1_r, 1_r, 1_p)}{4\sqrt{2}}. \end{aligned} \quad (4.21)$$

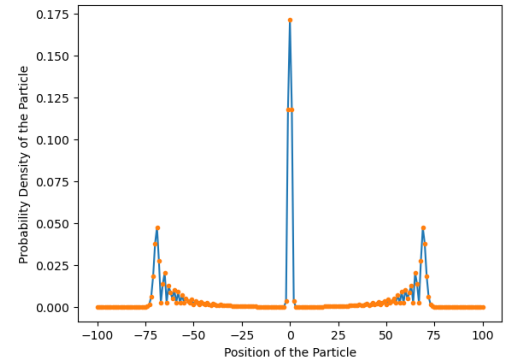
After N steps,

$$|\phi(N)\rangle = V_{ec}^N |\phi(initial)\rangle_{ec}. \quad (4.22)$$

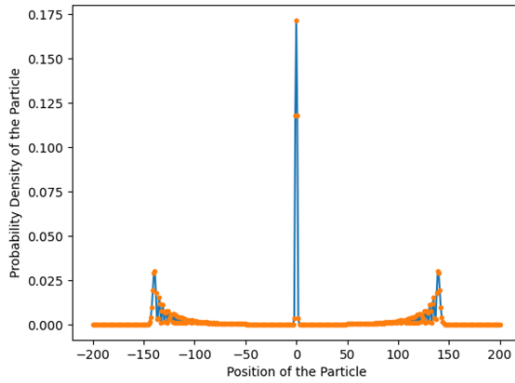
Now we perform measurements from eq.4.12 and the table 4.1 shows the probability values of positions for the maximally entangled coin quantum walk.



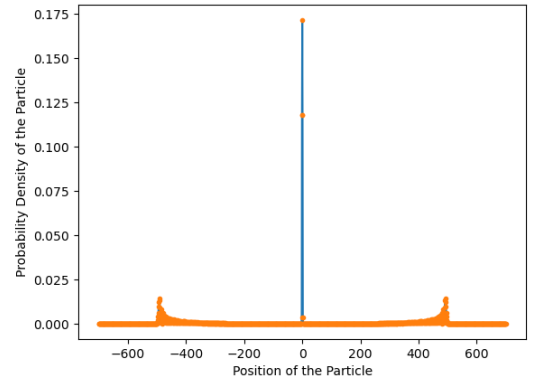
(a) $N=60$



(b) $N=100$



(c) $N=200$



(d) $N=700$

Figure 4.3: The probabilities of the walker after 60, 100, 200, 700 steps of the walk with a maximally entangled coin state are plotted against the positions where the walker can be located.

	Positions	-3	-2	-1	0	1	2	3
Probability	Step 0	0	0	0	1	0	0	0
	Step 1	0	0	1/2	0	1/2	0	0
	Step 2	0	1/8	2/8	2/8	2/8	1/8	0
	Step 3	1/32	6/32	5/32	8/32	5/32	6/32	1/32

Table 4.1: The probability distribution of the walker with maximally entangled coin state after first three steps of the walk. It suggests that entanglement produces symmetry in the distribution.

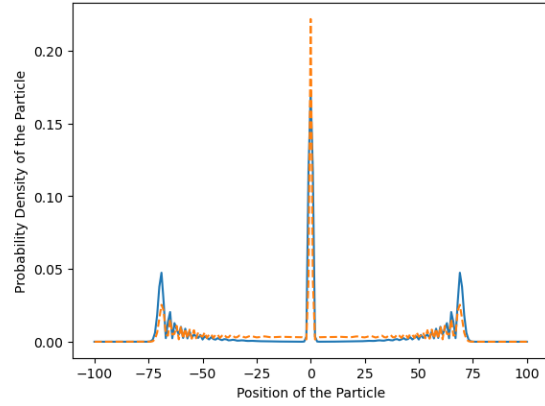
Simulating this walk for 60, 100, 200 and 700 steps yields the plot for the probability distribution of the walker corresponding to the positions on the line. Hitherto, we have seen that the probability distribution in case of CRW is binomial with greater probabilities at and around the origin and decreasing as we move sideways on the line. However, the quantum walk with a single coin or with two entangled coins exhibits much greater spread of probabilities across a multitude of positions. Also, the classical distribution had only one peak, on the contrary, the distribution in fig. 4.3 shows two more peaks as the walker propagates to the extreme points of the walk. We call this property as "the three peak zone". This distribution of position probabilities is advantageous in devising algorithms that are faster and more efficient than their classical analogues. Another coin that we can use is the fourier coin which is given as

$$\hat{F} = \frac{1}{\sqrt{2}}(|0\rangle\langle 0| + \iota|0\rangle\langle 1| + \iota|1\rangle\langle 0| + |1\rangle\langle 1|). \quad (4.23)$$

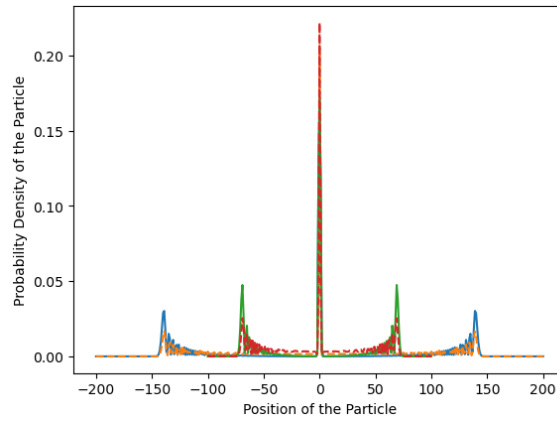
Our coin state is a bipartite state so we use $\hat{Y} = \hat{F} \otimes \hat{F}$ which is described as

$$\begin{aligned} \hat{Y} = \frac{1}{2} & (|00\rangle\langle 00| + \iota|01\rangle\langle 00| + \iota|10\rangle\langle 00| - |11\rangle\langle 00| \\ & + \iota|00\rangle\langle 01| + |01\rangle\langle 01| - |10\rangle\langle 01| + \iota|11\rangle\langle 01| \\ & + \iota|00\rangle\langle 10| - |01\rangle\langle 10| + |10\rangle\langle 10| + \iota|11\rangle\langle 10| \\ & - |00\rangle\langle 11| + \iota|01\rangle\langle 11| + \iota|10\rangle\langle 11| + |11\rangle\langle 11|). \end{aligned} \quad (4.24)$$

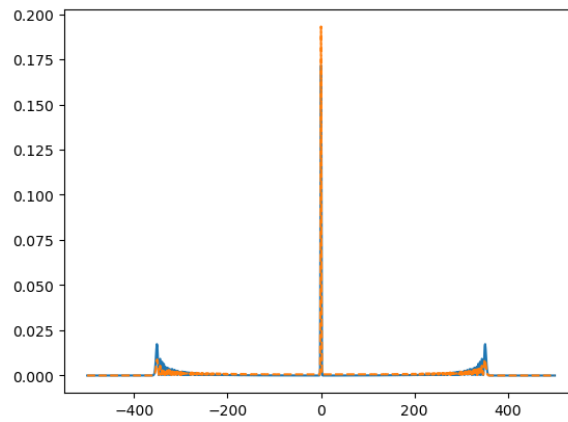
Now apply Unitary operator $V_{ec} = \hat{S} \cdot (\hat{Y} \otimes I_p)$ and apply the above process again so we can get the probability distribution for Fourier coin as compared to the Hadamard coin for 100 steps in fig. 4.4a. Let us now compare the effect of two coins i.e. Hadamard and Fourier on the first bell state for 100 and 200 steps in fig. 4.4b. The feature of three peak zone is again prominent. At the origin, the probability distribution is greater in both circumstances than it is in the classical example. The number of steps for red and green plots are 100 and for blue and orange plots are 200. The shift operator currently in use is the same as the one previously used (eq. 4.7) while coin operator for green and blue plot is given by eq. 4.6 and orange and red is given by eq. 4.24. There are more minor probabilities that accords to the areas between the two extreme



(a) $N=100$



(b) $N=100$ and $N=200$



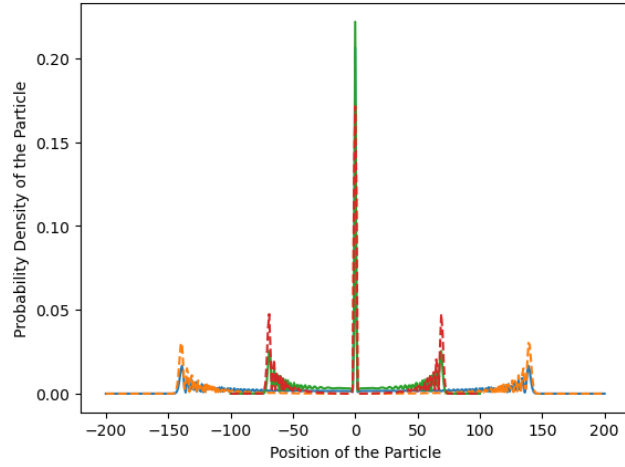
(c) $N=500$

Figure 4.4: The probabilities of the walker after 100, 200 and 500 steps of the walk with a First Bell state as coin state are plotted against the positions where the walker can be located. Coin operator for blue and green plots is given by eq.4.6 and dashed orange and red plots are given by 4.24

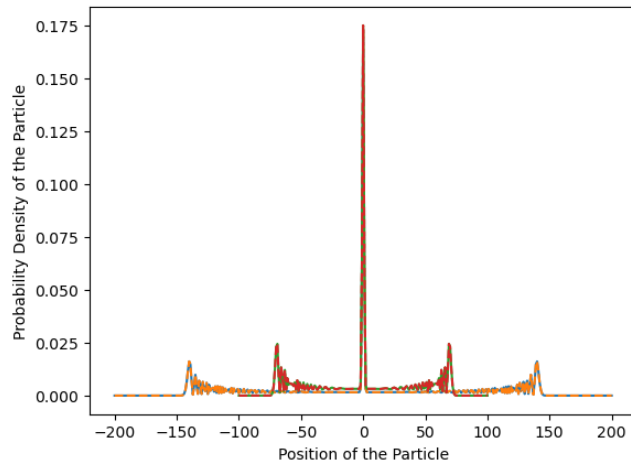
peaks and the middle one. Note that the peaks observed in both extreme zones are of a lesser magnitude for 500 steps (fig. 4.4c) in comparison to 200 steps, and notably decreased even further for 100 steps when compared to the 200 step scenario. We can also observe that relative to 100 steps, it is noticeable that 200 steps encompass a wider interval on the number line. Moreover, the span expands even further with 500 steps and this is the main reason behind extreme peaks of lesser magnitude. We can also plot similar plots for second and third bell states as in fig. 4.6a and fig. 4.6b, respectively. Note that the pattern of plots is same as for the first bell state however, the difference at peak values is observed. Observe that S (eq. 4.7) is a member of the family of permitted shift operators. For some of these operators, it may even be challenging to find a classical analogue because their existence is solely a product of quantum mechanics. One of these substitute operators is

$$\begin{aligned} \hat{S}' = & |00\rangle\langle 00| \otimes \sum_z |z+2\rangle\langle z| + |01\rangle\langle 01| \otimes \sum_z |z+1\rangle\langle z| \\ & + |10\rangle\langle 10| \otimes \sum_z |z-1\rangle\langle z| + |11\rangle\langle 11| \otimes \sum_z |z-2\rangle\langle z|. \end{aligned} \quad (4.25)$$

This shift operator specifies the transformation rules for the position of the particle in a quantum walk. When the state of the coin is $|00\rangle$ and $|11\rangle$, the particle position is incremented by 2 and decremented by 2, respectively. Meanwhile, when the state of the coin is $|01\rangle$ and $|10\rangle$, then the position is increased by 1 and decreased by 1, respectively. Now we use S' operator to observe the quantum walk. We can see that by using different shift operators, various types of result can be obtained that would be helpful in making new quantum algorithms. In order to explain the depth of quantum walk with entangled coins, we provide the graph depicted in fig. 4.6 (orange plot) which was created by using eq. 4.17 as a initial state, eq. 4.6 as a coin operator and eq. 4.25 as a shift operator. This graph is similar to the two-step quantum walk fig. 4.6 (dashed blue plot) with initial state $(\sqrt{0.85}|0\rangle - \sqrt{0.15}|1\rangle)_c \otimes |0\rangle_p$, eq. 4.6 as a coin operator and $\hat{S} = |0\rangle\langle 0| \sum_z |z+2\rangle\langle z| \otimes +|1\rangle\langle 1| \sum_z |z-2\rangle\langle z|$ as a shift operator. The number of steps are same in both the above cases (100 and 500). Depending on the elements of the coin state, the walker is compelled to take one or two steps in this situation.

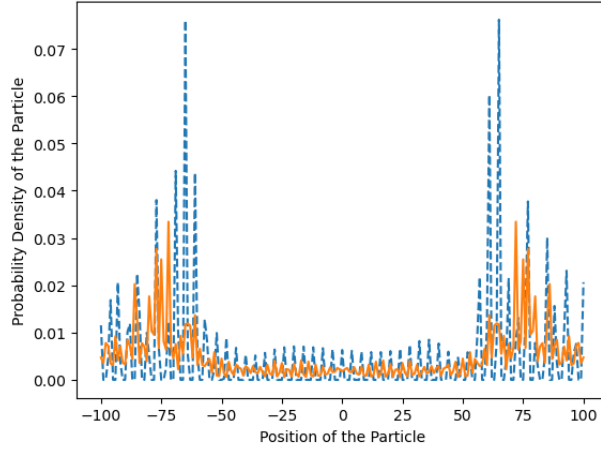


(a) Second Bell state (eq.2.22)

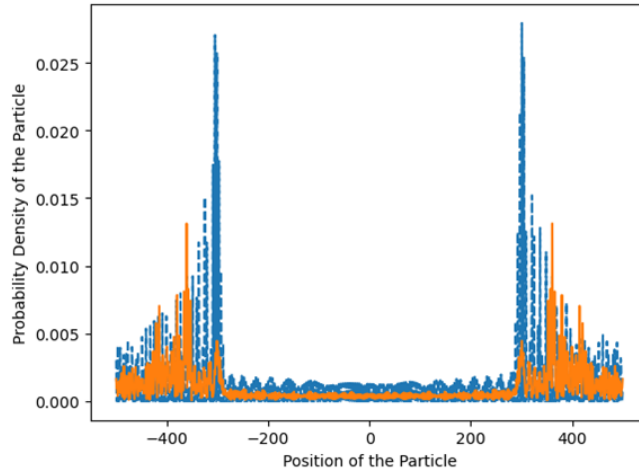


(b) Third Bell state (eq.2.23)

Figure 4.5: The probabilities of the walker after 100 and 200 steps of the walk with a Third Bell state as coin state are plotted against the positions where the walker can be located. Coin operator for red and blue plots are given by eq.4.6 and dashed orange and green plots are given by 4.24.



(a) $N=100$



(b) $N=500$

Figure 4.6: The probabilities of the walker after 100 and 500 steps of the walk with a first Bell state (orange dashed line) and $\sqrt{0.85}|0\rangle - \sqrt{0.15}|1\rangle$ (blue dashed line) as coin states are plotted against the positions where the walker can be located. Coin operator for red and blue plots are given by eq. 4.6 and dashed orange and green plots are given by 4.24.

The behaviour of quantum walk drastically alters as a result of the change in the shift operator. In this instance, constructive interference occurs in several sections of the graph.

Till now we have discussed the single coin with a single walker and also two coins with a single walker. Two coins can be separable, partially entangled or maximally entangled. In each case, we got different probability distributions. However, symmetric distributions are obtained in the case of superposition coin state and maximally entangled state. In the next section, another coin state is discussed i.e. coin state with complex coefficients in which we also got symmetric results as in the maximally entangled coin state.

4.4 Quantum Walk with Complex Coefficients in the Coin initial state

For instance, we take a coin with complex coefficients and initialize the state as

$$|\text{coin}\rangle_{com} = \frac{1}{2}(|0\rangle + \iota|1\rangle)_c(|0\rangle + \iota|1\rangle)_c. \quad (4.26)$$

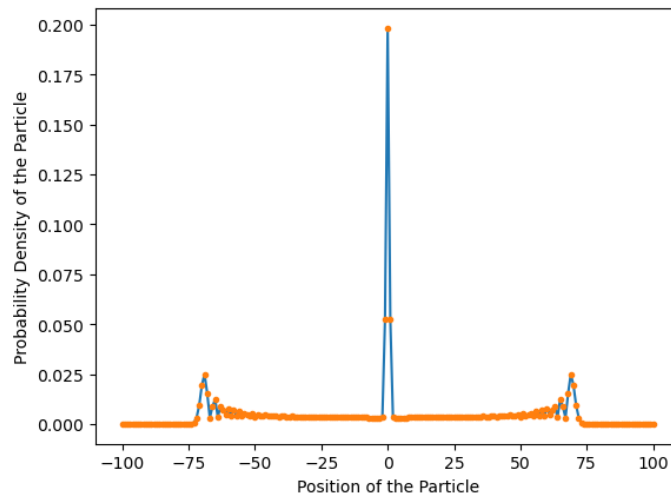
The particle is at origin so $|pos\rangle = |0\rangle_p$ and the initial state (from eq.3.18) of the composite would become,

$$|\phi(\text{initial})\rangle_{com} = |0\rangle_p \otimes \frac{1}{2}(|0\rangle + \iota|1\rangle)_c(|0\rangle + \iota|1\rangle)_c. \quad (4.27)$$

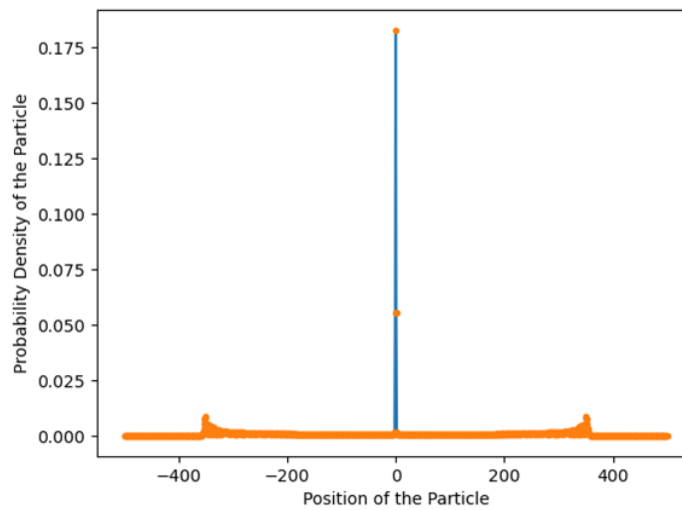
The evolution operator of the system we use is,

$$V_{com} = \hat{S} \cdot (\hat{G} \otimes I_p), \quad (4.28)$$

where \hat{G} and \hat{S} are taken from eq. 4.6 and eq. 4.7, respectively. The probability distribution that results when entanglement is used, has more symmetry (fig. 4.7). We would therefore get the probability distributions that estimates quantum walks with maximally entangled coins having unimaginary coefficients if we widened the initial conditions and allowed coins to be introduced with complex coefficients.



(a) $N=100$



(b) $N=500$

Figure 4.7: The probabilities of the walker after 100 steps of the walk with a complex coefficients in coin initial state are plotted against the positions where the walker can be located.

Chapter 5

Summary and Conclusion

In the introductory chapters of this thesis, the inception of the concept of entanglement is viewed and therein the advances that are made since are briefly discussed. A background of classical random walk and its limitations are presented, along with the details of Discrete Quantum Walk. The categorization of quantum states/ systems into pure and mixed is described with regards to the density operators. The concept of separability and entanglement comes therein after with a brief idea presented in the seminal paper of Einstein, Podolsky and Rosen [63]. Schmidt decomposition and Von Neumann Entropy are discussed as a pointer for the detection of entanglement. This thesis focused on Classical Walks leading to Quantum walks with several values of entanglement and compared their probability distributions. This provides a detailed analysis of the discrete time quantum walks on the unrestricted line, in particular, the coined (Hadamard and Fourier) quantum walk and using different shift operators. To probe the role of entanglement in quantum walks, the probability distribution of the walk is explored for separable states, states in superposition, and entangled states with varying amount of entanglement. It is seen that entanglement enriches the probability distribution of the walker. This property renders quantum walk a powerful tool to model computationally faster quantum algorithms. For several different operators of entangled coins, the fundamental "three-peak zone" form is repeated. We also pondered about how a quantum walk with coins under other circumstances specifically a non-entangled coin with complex coefficients could lead to "three-peak zone" form.

Depending on the particular coin used that is maximally entangled, the quantum walks with these coins demonstrate a range of quantitative behaviours (peaks that are greater or lower), despite the similarity in shape of both probability distributions. Our probability distributions can be symmetric thanks to entanglement without the need for complex coin state coefficients. In future, we can build new quantum algorithms by using different initial states, different coin operators and shift operators. We can have several probability distributions either symmetrical or non-symmetrical according to our need.

Bibliography

- [1] Boya, Luis J. "The thermal radiation formula of Planck (1900)." arXiv preprint physics/0402064 (2004)..
- [2] Niaz, Mansoor. Critical appraisal of physical science as a human enterprise: Dynamics of scientific progress. Vol. 36. Springer Science Business Media, 2009.
- [3] Bennett, Charles H., Gilles Brassard, and N. David Mermin. "Quantum cryptography without Bell's theorem." *Physical review letters* 68, no. 5 (1992): 557.
- [4] Ekert, Artur K. "Quantum cryptography based on Bell's theorem." *Physical review letters* 67, no. 6 (1991): 661.
- [5] Bennett, Charles H., and Stephen J. Wiesner. "Communication via one-and two-particle operators on Einstein-Podolsky-Rosen states." *Physical review letters* 69, no. 20 (1992): 2881.
- [6] Bennett, Charles H., Gilles Brassard, Claude Crépeau, Richard Jozsa, Asher Peres, and William K. Wootters. "Teleporting an unknown quantum state via dual classical and Einstein-Podolsky-Rosen channels." *Physical review letters* 70, no. 13 (1993): 1895.
- [7] Shor, Peter W. "Algorithms for quantum computation: discrete logarithms and factoring." In *Proceedings 35th annual symposium on foundations of computer science*, pp. 124-134. Ieee, 1994.
- [8] Farhi, Edward, and Sam Gutmann. "Quantum computation and decision trees." *Physical Review A* 58, no. 2 (1998): 915.

- [9] Childs, Andrew M., Edward Farhi, and Sam Gutmann. "An example of the difference between quantum and classical random walks." *Quantum Information Processing* 1 (2002): 35-43.
- [10] Moore, Cristopher, and Alexander Russell. "Quantum walks on the hypercube." In *International Workshop on Randomization and Approximation Techniques in Computer Science*, pp. 164-178. Berlin, Heidelberg: Springer Berlin Heidelberg, 2002.
- [11] Gerhardt, Heath, and John Watrous. "Continuous-time quantum walks on the symmetric group." In *International Workshop on Randomization and Approximation Techniques in Computer Science*, pp. 290-301. Berlin, Heidelberg: Springer Berlin Heidelberg, 2003.
- [12] Ahmadi, Amir, Ryan Belk, Christino Tamon, and Carolyn Wendler. "On mixing in continuous-time quantum walks on some circulant graphs." *Quantum Information Computation* 3, no. 6 (2003): 611-618.
- [13] Fedichkin, Leonid, Dmitry Solenov, and Christino Tamon. "Mixing and decoherence in continuous-time quantum walks on cycles." (2005).
- [14] Aharonov, Y. "L, Davidovich and N. Zagury." *Phys. Rev. A* 48, no. 2 (1993).
- [15] Meyer, David A. "From quantum cellular automata to quantum lattice gases." *Journal of Statistical Physics* 85 (1996): 551-574.
- [16] Nayak, Ashwin, and Ashvin Vishwanath. "Quantum walk on the line." (2000).
- [17] Aharonov D, Ambainis A, Kempe J and Vazirani U 2001 Quantum walks on graphs *Proc. 33th ACM Symp. on The Theory of Computing (New York)* pp 50–59
- [18] Brun, Todd A., Hilary A. Carteret, and Andris Ambainis. "Quantum to classical transition for random walks." *Physical review letters* 91, no. 13 (2003): 130602.

- [19] Jeong, Hyunseok, Mauro Paternostro, and Myungshik S. Kim. "Simulation of quantum random walks using the interference of a classical field." *Physical Review A* 69, no. 1 (2004): 012310.
- [20] Knight, Peter L., Eugenio Roldán, and John E. Sipe. "Propagating quantum walks: the origin of interference structures." *journal of modern optics* 51, no. 12 (2004): 1761-1777.
- [21] Childs, Andrew M., Richard Cleve, Enrico Deotto, Edward Farhi, Sam Gutmann, and Daniel A. Spielman. "Exponential algorithmic speedup by a quantum walk." In *Proceedings of the thirty-fifth annual ACM symposium on Theory of computing*, pp. 59-68. 2003.
- [22] Shenvi, Neil, Julia Kempe, and K. Birgitta Whaley. "Quantum random-walk search algorithm." *Physical Review A* 67, no. 5 (2003): 052307.
- [23] Ambainis, Andris, Eric Bach, Ashwin Nayak, Ashvin Vishwanath, and John Watrous. "One-dimensional quantum walks." In *Proceedings of the thirty-third annual ACM symposium on Theory of computing*, pp. 37-49. 2001.
- [24] Kempe, Julia. "Discrete quantum walks hit exponentially faster." In *International Workshop on Randomization and Approximation Techniques in Computer Science*, pp. 354-369. Berlin, Heidelberg: Springer Berlin Heidelberg, 2003.
- [25] Ambainis, Andris. "Quantum walk algorithm for element distinctness." *SIAM Journal on Computing* 37, no. 1 (2007): 210-239.
- [26] Kempe, J. "Quantum random walk algorithms." *Contemp. Phys* 44, no. 3 (2003): 302-327.
- [27] Ambainis, Andris. "Quantum walks and their algorithmic applications." *International Journal of Quantum Information* 1, no. 04 (2003): 507-518.
- [28] Brun, Todd A., Hilary A. Carteret, and Andris Ambainis. "Quantum walks driven by many coins." *Physical Review A* 67, no. 5 (2003): 052317.

- [29] Tregenna, Ben, Will Flanagan, Rik Maile, and Viv Kendon. "Controlling discrete quantum walks: coins and initial states." *New Journal of Physics* 5, no. 1 (2003): 83.
- [30] Ambainis, Andris, Julia Kempe, and Alexander Rivosh. "Coins make quantum walks faster." arXiv preprint quant-ph/0402107 (2004).
- [31] Kendon, Viv, and Ben Tregenna. "Decoherence can be useful in quantum walks." *Physical Review A* 67, no. 4 (2003): 042315.
- [32] Kendon, Viv, and Ben Tregenna. "Decoherence in discrete quantum walks." In *Decoherence and Entropy in Complex Systems: Selected Lectures from DICE 2002*, pp. 253-267. Berlin, Heidelberg: Springer Berlin Heidelberg, 2003.
- [33] Brun, Todd A., Hilary A. Carteret, and Andris Ambainis. "Quantum random walks with decoherent coins." *Physical Review A* 67, no. 3 (2003): 032304.
- [34] Mackay, Troy D., Stephen D. Bartlett, Leigh T. Stephenson, and Barry C. Sanders. "Quantum walks in higher dimensions." *Journal of Physics A: Mathematical and General* 35, no. 12 (2002): 2745.
- [35] Du, Jiangfeng, Hui Li, Xiaodong Xu, Mingjun Shi, Jihui Wu, Xianyi Zhou, and Rongdian Han. "Experimental implementation of the quantum random-walk algorithm." *Physical Review A* 67, no. 4 (2003): 042316.
- [36] Omar, Y., N. Paunković, L. Sheridan, and S. Bose. "Quantum walk on a line with two entangled particles." *Physical Review A* 74, no. 4 (2006): 042304.
- [37] Carneiro, Ivens, Meng Loo, Xibai Xu, Mathieu Girerd, Viv Kendon, and Peter L. Knight. "Entanglement in coined quantum walks on regular graphs." *New Journal of Physics* 7, no. 1 (2005): 156.
- [38] Endrejat, Jochen, and Helmut Buettner. "Entanglement measurement with discrete multiple-coin quantum walks." *Journal of Physics A: Mathematical and General* 38, no. 42 (2005): 9289.

- [39] Abal, G., R. Siri, A. Romanelli, and R. Donangelo. "Quantum walk on the line: Entanglement and nonlocal initial conditions." *Physical Review A* 73, no. 4 (2006): 042302.
- [40] Sanders, Barry C., Stephen D. Bartlett, Ben Tregenna, and Peter L. Knight. "Quantum quincunx in cavity quantum electrodynamics." *Physical Review A* 67, no. 4 (2003): 042305.
- [41] Travaglione, Ben C., and Gerald J. Milburn. "Implementing the quantum random walk." *Physical Review A* 65, no. 3 (2002): 032310.
- [42] Rowe, Mary A., David Kielpinski, Volker Meyer, Charles A. Sackett, Wayne M. Itano, Christopher Monroe, and David J. Wineland. "Experimental violation of a Bell's inequality with efficient detection." *Nature* 409, no. 6822 (2001): 791-794.
- [43] Plenio, Martin B., S. F. Huelga, A. Beige, and P. L. Knight. "Cavity-loss-induced generation of entangled atoms." *Physical Review A* 59, no. 3 (1999): 2468.
- [44] Le Bellac, Michel. *A short introduction to quantum information and quantum computation*. Cambridge University Press, 2006.
- [45] Giovannetti, Vittorio, Stefano Mancini, David Vitali, and Paolo Tombesi. "Characterizing the entanglement of bipartite quantum systems." *Physical Review A* 67, no. 2 (2003): 022320.
- [46] Blum, Karl. *Density matrix theory and applications*. Vol. 64. Springer Science Business Media, 2012.
- [47] Gerry, Christopher, and Peter L. Knight. *Introductory quantum optics*. Cambridge university press, 2005.
- [48] Krammer, Philipp. *Quantum entanglement: Detection, classification, and quantification*. na, 2005. .

- [49] Brassard, Gilles, and André Allan Méthot. "Can quantum-mechanical description of physical reality be considered in complete?." *International Journal of Quantum Information* 4, no. 01 (2006): 45-54.
- [50] V. Vedral, "Quantum entanglement," *Nature Physics*, vol. 10, no. 4, pp. 256–258, 2014.
- [51] Zou, Nanxi. "Quantum entanglement and its application in quantum communication." In *Journal of Physics: Conference Series*, vol. 1827, no. 1, p. 012120. IOP Publishing, 2021.
- [52] Gu, Xuemei, Lijun Chen, and Mario Krenn. "Quantum experiments and hypergraphs: Multiphoton sources for quantum interference, quantum computation, and quantum entanglement." *Physical Review A* 101, no. 3 (2020): 033816.
- [53] Horodecki, Ryszard, Paweł Horodecki, Michał Horodecki, and Karol Horodecki. "Quantum entanglement." *Reviews of modern physics* 81, no. 2 (2009): 865.
- [54] Augusiak, Remigiusz, J. Kołodyński, Alexander Streltsov, Manabendra Nath Bera, Antonio Acin, and Maciej Lewenstein. "Asymptotic role of entanglement in quantum metrology." *Physical Review A* 94, no. 1 (2016): 012339.
- [55] Nielsen, Michael A., and Isaac L. Chuang. *Quantum computation and quantum information*. Cambridge university press, 2010.
- [56] Kak, Subhash. "Quantum information and entropy." *International Journal of Theoretical Physics* 46 (2007): 860-876.
- [57] Terhal, Barbara M., and Paweł Horodecki. "Schmidt number for density matrices." *Physical Review A* 61, no. 4 (2000): 040301.
- [58] Chernov, N., and D. Dolgopyat. "Diffusive motion and recurrence on an idealized Galton Board." *Physical review letters* 99, no. 3 (2007): 030601.
- [59] Portugal, Renato. *Quantum walks and search algorithms*. Vol. 19. New York: Springer, 2013.

- [60] Kadian, Karuna, Sunita Garhwal, and Ajay Kumar. "Quantum walk and its application domains: A systematic review." *Computer Science Review* 41 (2021): 100419.
- [61] Aharonov, Yakir, Luiz Davidovich, and Nicim Zagury. "Quantum random walks." *Physical Review A* 48, no. 2 (1993): 1687.
- [62] Farhi, Edward, and Sam Gutmann. "Quantum computation and decision trees." *Physical Review A* 58, no. 2 (1998): 915.
- [63] Reid, M. D., P. D. Drummond, W. P. Bowen, Eric Gama Cavalcanti, Ping Koy Lam, H. A. Bachor, Ulrik Lund Andersen, and G. Leuchs. "Colloquium: the Einstein-Podolsky-Rosen paradox: from concepts to applications." *Reviews of Modern Physics* 81, no. 4 (2009): 1727.